Acta Crystallographica Section B
Structural Science
ISSN 0108-7681

Salts of maleic and fumaric acids with organic polyamines: comparison of isomeric acids as building blocks in supramolecular chemistry

Katharine F. Bowes,[a] George Ferguson,[b] Alan J. Lough[c] and Christopher Glidewell[a]*

[a]School of Chemistry, University of St Andrews, St Andrews, Fife KY16 9ST, Scotland, UK, [b]Department of Chemistry, University of Guelph, Guelph, Ontario, Canada N1G 2W1, and [c]Lash Miller Chemical Laboratories, University of Toronto, Toronto, Ontario, Canada M5S 3H6

Correspondence e-mail: cg@st-andrews.ac.uk

Received 22 October 2002
Accepted 6 November 2002

Maleic acid and fumaric acid both readily form adducts with organic diamines: maleic acid usually forms 2:1 adducts with bases, while fumaric acid usually forms 1:1 adducts, and the supramolecular stuctures within the two series are not simply related. The 1:2 adducts formed by 1,2-bis(4-pyridyl)ethane and by 4,4′-bipyridyl, respectively, with maleic acid, compounds (1) and (2), are salts $[\{(\text{diamine})H_2\}^{2+}]\cdot[(C_4H_3O_4)^-]_2$ in which the cations lie across a centre of inversion and a twofold rotation axis, respectively. The ions are linked by N—H···O hydrogen bonds into three-ion aggregates, which are further linked by C—H···O hydrogen bonds into two- and three-dimensional arrays, respectively. In the fumarate salts formed by 2,2′-dipyridylamine (1:1) and 1,4-diazabicyclo[2.2.2]octane (1:2), compounds (3) and (4), the ionic components are linked into molecular ladders. The 1:1 adduct of 4,4′-bipyridyl and fumaric acid, compound (5), contains two neutral components, both of which lie across centres of inversion; these components are linked into chains by a single O—H···N hydrogen bond and thence into sheets by C—H···O hydrogen bonds. The corresponding adduct formed by 1,4-diazabicyclo[2.2.2]-octane, compound (6), is a salt that again contains chains linked into sheets by C—H···O hydrogen bonds. In the 1:1 adducts, compounds (7), (8) and (10), that are formed between 1,2-bis(4-pyridyl)ethane, 4,4′-trimethylenedipyridine and hexamethylenetetramine, respectively, with fumaric acid, and in the 1:2 adduct, compound (9), of 2,2′-dipyridylamine and maleic acid, the chains that are generated by the hard hydrogen bonds are linked by C—H···O hydrogen bonds to form, in each case, a single three-dimensional framework. In the 1:1 adduct, compound (11), of 2,2′-bipyridyl and fumaric acid the hydrogen bonds generate two interwoven three-dimensional frameworks.

1. Introduction

In hydrogen-bonded adducts of simple bis-phenols or dicarboxylic acids with tertiary diamines, the primary mode of supramolecular aggregation is chain formation by hard (Braga *et al.*, 1995) O—H···N and/or N—H···O hydrogen bonds (Coupar *et al.*, 1997; Ferguson *et al.*, 1997, 1998; Glidewell *et al.*, 1999; Lavender *et al.*, 1999). The mutual disposition of the hydrogen-bonded chains is often determined by soft (Braga *et al.*, 1995) hydrogen bonds, usually of C—H···O type, or by aromatic $\pi\cdots\pi$ stacking interactions.

We have recently demonstrated, by the use of tartaric and malic acids (Farrell *et al.*, 2002*a*,*b*), that with a given range of diamines the corresponding adducts formed by enantiopure and racemic acids not only crystallize in different space groups

but often exhibit different supramolecular structures; indeed, in some cases different stoichiometries are also observed. The adducts formed by the enantiopure acids cannot normally crystallize in centrosymmetric space groups, in the absence of considerable disorder, while the adducts formed by the racemic acids invariably crystallize in centrosymmetric space groups, as the occurrence of inversion centres, especially unoccupied inversion centres, seems to be particularly favourable in molecular crystals (Brock & Dunitz, 1994). Continuing our exploration of the influence of molecular configuration on space group, and hence of the molecular configuration's influence on supramolecular structure, we have now turned to a *cis* and *trans* pair of dicarboxylic acids, maleic acid and fumaric acid ($C_4H_4O_4$), the *Z* and *E* isomers, respectively, of 1,4-but-2-enedioic acid. In principle, a neutral molecule of fumaric acid and its dianion could lie across inversion centres and/or twofold rotation axes with local symmetry as high as C_{2h} (2/*m*), while neutral maleic acid and its dianion could lie across a twofold rotation axis with local symmetry as high as C_{2v} (*mm*2). While the molecules in pure maleic acid lie in general positions in space group $P2_1/c$ (Shahat, 1952; James & Williams, 1974), in both the monoclinic (α) polymorph of fumaric acid (Brown, 1966) and the triclinic (β) form (Bednowitz & Post, 1966) molecules lie across inversion centres, with $Z' = 1.5$ in $P2_1/c$ and $Z' = 0.5$ in $P\overline{1}$.

Here we report the structures of a number of the adducts formed by maleic acid (*A*) and fumaric acid (*B*) with a range of cognate organic diamines (Scheme I): 1,2-bis-(4-pyridyl)ethane (*C*), 4,4′-bipyridyl (*D*), 2,2′-dipyridylamine (*E*), 1,4-diazabicyclo[2.2.2]octane (DABCO) (*F*), 4,4′-trimethylenedipyridine (*G*), hexamethylenetetramine (HMTA) (*H*) and 2,2′-bipyridyl (*J*).

The products described here are 1,2-bis(4-pyridyl)ethane–maleic acid (1/2), $C_{12}H_{12}N_2\cdot(C_4H_4O_4)_2$ (1); 4,4′-bipyridyl–maleic acid (1/2), $C_{10}H_8N_2\cdot(C_4H_4O_4)_2$ (2); 2,2′-dipyridylamine–fumaric acid (1/1), $C_{10}H_9N_3\cdot C_4H_4O_4$ (3); DABCO–fumaric acid (1/2), $C_6H_{12}N_2\cdot(C_4H_4O_4)_2$ (4); 4,4′-bipyridyl–fumaric acid (1/1), $C_{10}H_8N_2\cdot C_4H_4O_4$ (5); DABCO–fumaric acid (1/1), $C_6H_{12}N_2\cdot C_4H_4O_4$ (6); 1,2-bis(4-pyridyl)ethane–fumaric acid (1/1), $C_{12}H_{12}N_2\cdot C_4H_4O_4$ (7); 4,4′-trimethylenedipyridine–fumaric acid (1/1), $C_{13}H_{14}N_2\cdot C_4H_4O_4$ (8); 2,2′-dipyridylamine–maleic acid (1/2), $C_{10}H_9N_3\cdot(C_4H_4O_4)_2$ (9); HMTA–fumaric acid (1/1), $C_6H_{12}N_4\cdot C_4H_4O_4$ (10); and 2,2′-bipyridyl–fumaric acid, $C_{10}H_8N_2\cdot C_4H_4O_4$ (11).

The structures of (2) and (5) have been reported briefly in a proof of constitution study (Chatterjee *et al.*, 1998) but very few details were given. In particular, the numbers of data and of refined parameters were not specified, so any evaluation of the reported *R* factors is precluded; the twofold rotational symmetry of the bipyridyl unit in (2) and the inversion symmetry of the acid unit in (5) were not mentioned, nor was there any indication of how the H atoms had been located; and, more important in the present context, this earlier report contained no description or analysis of the supramolecular aggregation patterns. Accordingly, we have reinvestigated these two compounds as part of this study, and we give a full structural description and analysis for each. However, Sun & Jin (2002) have recently presented a detailed description of the supramolecular structure of the salt-type 1:2 adduct formed by DABCO with maleic acid: below we compare this structure with the analogous adducts formed between DABCO and fumaric acid.

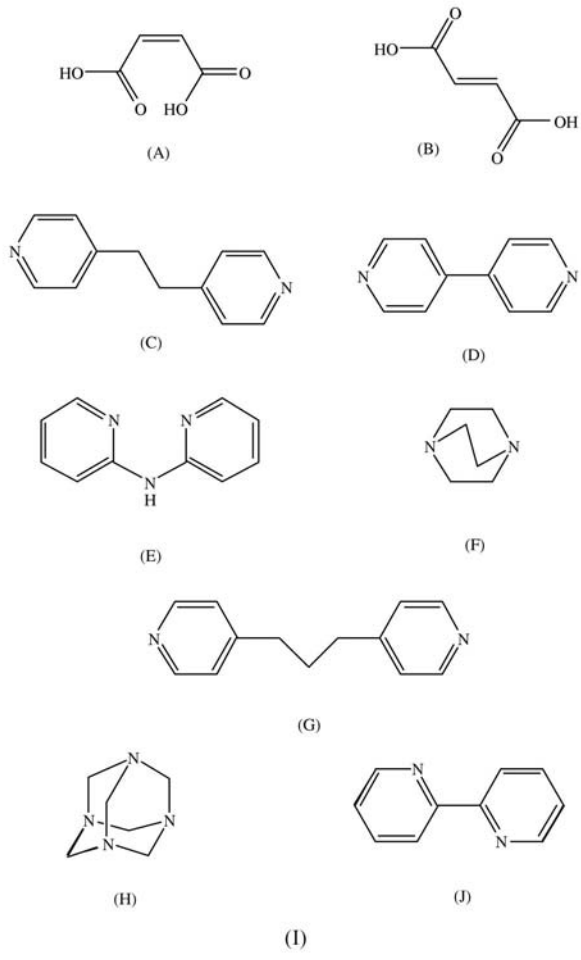

2. Experimental

2.1. Synthesis

Stoichiometric quantities of the two components (amine-to-acid molar ratios of 1:1 and 1:2 were employed) were separately dissolved in methanol. The solutions were mixed and then set aside to crystallize. Analytically pure (1)–(9) and (11) were produced. Analyses: (1) found C 57.9, H 4.5, N 6.6%; $C_{20}H_{20}N_2O_8$ requires C 57.7, H 4.8, N 6.7%; (2) found C 55.7, H 3.8, N 7.2%; $C_{18}H_{16}N_2O_8$ requires C 55.7, H 4.2, N 7.2%; (3) found C 58.3, H 4.4, N 14.7%; $C_{14}H_{13}N_3O_4$ requires C 58.5, H 4.6, N 14.6%; (4) found C 48.9, H 5.9, N 8.1%; $C_{14}H_{20}N_2O_8$ requires C 48.8, H 5.9, N 8.1%; (5) found C 61.8, H 3.8, N 10.3%; $C_{14}H_{12}N_2O_4$ requires C 61.8, H 4.4, N 10.3%; (6) found C 52.6, H 7.3, N 12.3%; $C_{10}H_{16}N_2O_4$ requires C 52.6, H 7.1, N 12.3%; (7) found C 63.5, H 5.3, N 9.2%; $C_{16}H_{16}N_2O_4$

requires C 64.0, H 5.4, N 9.3%; (8) found C 64.8, H 5.9, N 8.9%; $C_{17}H_{18}N_2O_4$ requires C 65.0, H 5.8, N 8.9%; (9) found C 53.9, H 4.0, N 10.5%; $C_{18}H_{17}N_3O_8$ requires C 53.6, H 4.2, N 10.4%; (11) found C 61.6, H 4.1, N 10.3%; $C_{14}H_{12}N_2O_4$ requires C 61.8, H 4.4, N 10.3%. Crystals of (1)–(9) and (11) that were suitable for single-crystal X-ray diffraction were selected directly from the analytical samples.

The reaction of fumaric acid with HMTA yielded predominantly $[(NH_4)^+]\cdot[(C_4H_3O_4)^-]$, ammonium hydrogenfumarate, which was identified both by elemental analysis (found C 36.5, H 5.1, N 10.5%; $C_4H_7NO_4$ requires C 36.1, H 5.3, N 10.5%) and by comparison of its unit-cell dimensions with literature values (Yardley, 1925). A few crystals of a 1:1 adduct of HMTA and fumaric acid were isolated from this reaction product, but this adduct, (10), unexpectedly contained a mixture of fumaric acid and the saturated analogue succinic acid. It did not prove possible to collect a satisfactory dataset for the ammonium hydrogenfumarate. In addition we have prepared a 1:1 adduct of 1,2-bis(4-pyridyl)-ethene and fumaric acid, but in all preparations the crystals have been exceedingly small (analysis: found C 64.3, H 4.3, N 9.4; $C_{16}H_{14}N_2O_4$ requires C 64.4, H 4.7, N 9.4%). Attempts to prepare an analytically pure adduct of 2,2′-bipyridyl with maleic acid were thwarted by the formation of highly coloured by-products whose identity has not been pursued.

2.2. Data collection, structure solution and refinement

Diffraction data for (1)–(11) were collected at 150 (1) K using a Nonius Kappa-CCD diffractometer with graphite-monochromated Mo $K\alpha$ radiation ($\lambda = 0.71073$ Å). Other details of cell data, data collection and refinement are summarized in Table 1, together with details of the software employed.

Compounds (1), (3) and (5) are all triclinic, and the space group $P\overline{1}$ was selected and confirmed by the analysis for each compound. For (2), (4), (7) and (8) the systematic absences permitted Cc or $C2/c$ as possible space groups. In each case $C2/c$ was selected and confirmed by the analysis. The systematic absences permitted the unique assignment of space group $P2_1/c$ for (6) and (10) and of $P2_1/n$ for (9). For (11) the systematic absences permitted $Pca2_1$ and $Pcam$ (= $Pbcm$, No. 57) as possible space groups. $Pca2_1$ was selected and confirmed by the analysis. The structures were solved by direct methods and refined with all data on F^2. A weighting scheme based on $P = (F_o^2 + 2F_c^2)/3$ was employed in order to reduce statistical bias (Wilson, 1976).

Only in (3), (6), (10) and (11) do both components lie in general positions. In (1) the cation $[\{(C_{12}H_{12}N_2)H_2\}^{2+}]$ lies across an inversion centre, while in each of (5) and (7) both of the components lie across inversion centres. In (2) the cation $[\{(C_{10}H_8N_2)H_2\}^{2+}]$ lies across a twofold rotation axis; in (8) the diamine lies across a twofold rotation axis, while the acid lies across an inversion centre; and in (4) the cation $[\{(C_6H_{12}N_2)H_2\}^{2+}]$ lies across a twofold rotation axis. In (9) the cation is disordered across an inversion centre in $P2_1/n$, although it proved possible to solve and refine the structure of (9) in space group Pn, where the cation disorder was characterized by site-occupancy factors of 0.760 (15) and 0.240 (15) rather than 0.50 for each orientation. Despite the satisfactorily low R index in Pn (0.044 for 268 parameters and 2006 data) and the fact that the supramolecular structure is essentially the same as that found in $P2_1/n$, there were some unsatisfactory features in the difference maps, and this solution was accordingly rejected. In (10) it was apparent from an early stage that the acid component, which we expected to be derived from fumaric acid $C_4H_4O_4$, was in fact derived from a mixture of fumaric and its reduction product succinic acid, $C_4H_6O_4$. The terminal O atoms of these two components occupied very similar sites, while the central C atoms were necessarily in rather different sites because of the different conformational constraints. The refined site-occupancy factors were 0.726 (4) for the fumaric component and 0.274 (4) for the succinic component. For (11), with space group $Pca2_1$, the value of the Flack parameter (Flack, 1983), −0.5 (11), was inconclusive (Flack & Bernardinelli, 2000), and hence the Friedel equivalents were merged prior to the final refinements. All H atoms were located from difference maps and included in the refinements as riding atoms with distances O—H 0.84, N—H 0.88–0.93 and C—H 0.95–0.99.

Supramolecular analyses were performed and the diagrams were prepared with the aid of *PLATON* (Spek, 2002). Details of hydrogen-bond dimensions and of molecular conformations are given in Tables 2 and 3, and the bond distances for the cation in (10) are given in Table 4.[1] Figs. 1–29 show the molecular components, the atom-labelling schemes and aspects of the supramolecular structures.

3. Results and discussion

3.1. Crystallization characteristics and molecular constitutions

Regardless of whether the initial molar ratio of diamine to acid was 1:1 or 1:2, in general, maleic acid adducts crystallized with a 1:2 ratio of diamine to acid in the final product, while fumaric acid adducts had 1:1 stoichiometry. The sole exception to this stoichiometric generalization occurred with DABCO where solutions that contained 1:1 and 1:2 ratios of diamine to acid yielded crystalline adducts (6) and (4), respectively, which had stoichiometries identical to those of the starting solutions. The other unexpected observation was the crystallization of a 1:1 fumaric acid adduct from solutions that contained either a 1:1 or a 1:2 molar ratio of 4,4′-trimethylenedipyridine and maleic acid. Such an isomerization of maleic acid to fumaric acid has been observed previously in the presence of 4,4′-bipyridyl, although that isomerization did not occur in methanol solution but only in solutions in dimethylformamide or dimethylsulfoxide (Chatterjee *et al.*, 1998). We have so far been unable to synthesize an adduct of 4,4′-trimethylenedipyridine with maleic acid. The reaction of fumaric acid with

[1] Supplementary data for this paper are available from the IUCr electronic archives (Reference: NA0143). Services for accessing these data are described at the back of the journal.

Table 1
Experimental details.

	(1)	(2)	(3)	(4)	(5)
Crystal data					
Chemical formula	$C_{12}H_{14}N_2\cdot2(C_4H_3O_4)$	$C_{10}H_{10}N_2\cdot2(C_4H_3O_4)$	$C_{10}H_{10}N_3\cdot C_4H_3O_4$	$C_6H_{14}N_2\cdot2(C_4H_3O_4)$	$C_{10}H_8N_2\cdot C_4H_4O_4$
Chemical components†	*C*·2*A*	*D*·2*A*	*E*·*B*	*F*·2*B*	*D*·*B*
Chemical formula weight	416.38	388.33	287.27	344.32	272.26
Cell setting, space group	Triclinic, $P\overline{1}$	Monoclinic, $C2/c$	Triclinic, $P\overline{1}$	Monoclinic, $C2/c$	Triclinic, $P\overline{1}$
a, b, c (Å)	5.7958 (3), 9.4489 (6), 9.6031 (7)	24.0370 (16), 6.7434 (6), 11.4388 (10)	8.0021 (4), 8.7178 (4), 10.8497 (4)	20.1118 (9), 6.4737 (4), 12.5409 (7)	3.8040 (2), 8.8743 (5), 9.8764 (6)
α, β, γ (°)	86.787 (3), 73.010 (3), 76.986 (3)	90, 116.001 (4), 90	106.257 (3), 109.127 (3), 98.662 (2)	90, 115.070 (2), 90	109.757 (2), 97.246 (3), 96.813 (3)
V (Å^3)	490.01 (5)	1666.5 (2)	661.55 (6)	1478.97 (14)	306.59 (3)
Z, Z'	1, 0.5	4, 0.5	2, 1	4, 0.5	1, 0.5
D_x (Mg m^{-3})	1.411	1.548	1.442	1.546	1.475
Radiation type	Mo $K\alpha$	Mo $K\alpha$	Mo $K\alpha$	Mo $K\alpha$	Mo $K\alpha$
No. of reflections for cell parameters	2236	1888	3020	3025	1376
θ range (°)	3.1–27.6	3.5–27.5	2.7–27.4	3.3–27.5	2.7–27.5
μ (mm^{-1})	0.11	0.12	0.11	0.13	0.11
Temperature (K)	150 (1)	150 (1)	150 (1)	150 (1)	150 (1)
Crystal form, colour	Plate, colourless	Plate, colourless	Plate, colourless	Needle, colourless	Block, colourless
Crystal size (mm)	0.28 × 0.26 × 0.06	0.40 × 0.30 × 0.07	0.30 × 0.14 × 0.08	0.30 × 0.10 × 0.08	0.30 × 0.28 × 0.25
Data collection					
Diffractometer	Kappa–CCD	Kappa–CCD	Kappa–CCD	Kappa–CCD	Kappa–CCD
Data collection method	φ scans, and ω scans with κ offsets	φ scans, and ω scans with κ offsets	φ scans, and ω scans with κ offsets	φ scans, and ω scans with κ offsets	φ scans, and ω scans with κ offsets
Absorption correction	Multi-scan	Multi-scan	Multi-scan	Multi-scan	Multi-scan
T_{min}	0.968	0.877	0.889	0.956	0.945
T_{max}	0.991	0.995	0.989	0.995	0.978
No. of measured, independent and observed reflections	5489, 2236, 1676	6178, 1888, 1421	9473, 3020, 2028	5858, 1691, 1182	3277, 1376, 1105
Criterion for observed reflections	$I > 2\sigma(I)$	$I > 2\sigma(I)$	$I > 2\sigma(I)$	$I > 2\sigma(I)$	$I > 2\sigma(I)$
R_{int}	0.044	0.072	0.067	0.10	0.032
θ_{max} (°)	27.58	27.50	27.44	27.51	27.50
Range of h, k, l	$-7 \rightarrow h \rightarrow 7$ $-12 \rightarrow k \rightarrow 12$ $-11 \rightarrow l \rightarrow 12$	$-30 \rightarrow h \rightarrow 30$ $-8 \rightarrow k \rightarrow 8$ $-14 \rightarrow l \rightarrow 14$	$-10 \rightarrow h \rightarrow 10$ $-11 \rightarrow k \rightarrow 11$ $-14 \rightarrow l \rightarrow 14$	$-26 \rightarrow h \rightarrow 25$ $-6 \rightarrow k \rightarrow 8$ $-16 \rightarrow l \rightarrow 16$	$-4 \rightarrow h \rightarrow 4$ $-11 \rightarrow k \rightarrow 10$ $-12 \rightarrow l \rightarrow 12$
Intensity decay (%)	0	0	0	0	0
Refinement					
Refinement on	F^2	F^2	F^2	F^2	F^2
$R[F^2>2\sigma(F^2)]$, $wR(F^2)$, S	0.043, 0.121, 1.03	0.044, 0.119, 1.03	0.046, 0.130, 1.05	0.055, 0.156, 1.03	0.043, 0.125, 1.05
No. of reflections and parameters used in refinement	2236, 137	1888, 129	3020, 192	1691, 119	1376, 92
H-atom treatment	H-atom parameters constrained	H-atom parameters constrained	H-atom parameters constrained	H-atom parameters constrained	H-atom parameters constrained
Weighting scheme	$w = 1/[\sigma^2(F_o^2) + (0.0493P)^2 + 0.1138P]$ where $P = (F_o^2 + 2F_c^2)/3$	$w = 1/[\sigma^2(F_o^2) + (0.0462P)^2 + 1.0798P]$ where $P = (F_o^2 + 2F_c^2)/3$	$w = 1/[\sigma^2(F_o^2) + (0.0572P)^2 + 0.037P]$ where $P = (F_o^2 + 2F_c^2)/3$	$w = 1/[\sigma^2(F_o^2) + (0.0784P)^2 + 0.3794P]$ where $P = (F_o^2 + 2F_c^2)/3$	$w = 1/[\sigma^2(F_o^2) + (0.0681P)^2 + 0.0475P]$ where $P = (F_o^2 + 2F_c^2)/3$
$(\Delta/\sigma)_{max}$	<0.001	<0.001	<0.001	<0.001	<0.001
$\Delta\rho_{max}$, $\Delta\rho_{min}$ (e Å^{-3})	0.23, −0.18	0.24, −0.26	0.31, −0.28	0.30, −0.41	0.33, −0.23
Extinction method	*SHELXL*	*SHELXL*	*SHELXL*	*SHELXL*	None
Extinction coefficient	0.061 (15)	0.016 (3)	0.021 (5)	0.006 (2)	0

	(6)	(7)	(8)	(9)	(10)	(11)
Crystal data						
Chemical formula	$C_6H_{13.57}N_2\cdot\cdot C_4H_{2.43}O_4$	$C_{12}H_{12}N_2\cdot C_4H_4O_4$	$C_{13}H_{14}N_2\cdot C_4H_4O_4$	$C_{10}H_{10}N_3\cdot C_8H_7O_8$	$C_6H_{12}N_4\cdot\cdot 0.726(C_4H_4O_4)\cdot\cdot 0.274(C_4H_6O_4)$	$C_{10}H_8N_2\cdot C_4H_4O_4$
Chemical components†	*F*·*B*	*C*·*B*	*G*·*B*	*E*·2*A*	*H*·*B*	*J*·*B*
Chemical formula weight	228.25	300.31	314.33	403.35	256.82	272.26

Table 1 (continued)

	(6)	(7)	(8)	(9)	(10)	(11)
Cell setting, space group	Monoclinic, $P2_1/c$	Monoclinic, $C2/c$	Monoclinic, $C2/c$	Monoclinic, $P2_1/n$	Monoclinic, $P2_1/c$	Orthorhombic, $Pca2_1$
a, b, c (Å)	9.6845 (2), 8.8805 (2), 12.5886 (2)	21.0296 (14), 4.7456 (3), 16.6875 (11)	22.4349 (15), 4.6045 (3), 17.1156 (12)	11.566 (2), 5.4392 (11), 14.334 (3)	6.2877 (2), 15.9241 (6), 11.3315 (5)	23.9702 (6), 3.7416 (1), 14.8372 (4)
α, β, γ (°)	90, 100.0697 (15), 90	90, 118.394 (3), 90	90, 116.465 (3), 90	90, 99.03 (3), 90	90, 93.8556 (13), 90	90, 90, 90
V (Å^3)	1065.98 (4)	1465.03 (17)	1582.79 (18)	890.6 (3)	1132.01 (7)	1330.70 (6)
Z, Z'	4, 1	4, 0.5	4, 0.5	2, 0.5	4, 1	4, 1
D_x (Mg m^{-3})	1.422	1.362	1.319	1.504	1.504	1.359
Radiation type	Mo $K\alpha$	Mo $K\alpha$	Mo $K\alpha$	Mo $K\alpha$	Mo $K\alpha$	Mo $K\alpha$
No. of reflections for cell parameters	8844	1653	4202	2003	2583	8494
θ range (°)	2.8–27.5	2.8–27.5	3.7–27.5	2.9–27.4	2.6–27.5	3.2–27.5
μ (mm^{-1})	0.11	0.10	0.10	0.12	0.12	0.10
Temperature (K)	150 (1)	150 (1)	150 (1)	150 (1)	150 (1)	150 (1)
Crystal form, colour	Needle, colourless	Needle, colourless	Needle, colourless	Block, colourless	Plate, colourless	Needle, colourless
Crystal size (mm)	0.32 × 0.20 × 0.16	0.28 × 0.16 × 0.12	0.10 × 0.06 × 0.04	0.15 × 0.10 × 0.05	0.36 × 0.34 × 0.05	0.26 × 0.20 × 0.20
Data collection						
Diffractometer	Kappa–CCD	Kappa–CCD	Kappa–CCD	Kappa–CCD	Kappa–CCD	Kappa–CCD
Data collection method	φ scans, and ω scans with κ offsets	φ scans, and ω scans with κ offsets	φ scans, and ω scans with κ offsets	φ scans, and ω scans with κ offsets	φ scans, and ω scans with κ offsets	φ scans, and ω scans with κ offsets
Absorption correction	Multi-scan	Multi-scan	None	Multi-scan	Multi-scan	Multi-scan
T_{min}	0.966	0.963	–	0.980	0.913	0.901
T_{max}	0.982	0.987	–	0.994	0.996	0.981
No. of measured, independent and observed reflections	9143, 2430, 2007	4699, 1653, 1247	5661, 1782, 1240	5891, 2003, 1476	16012, 2583, 1686	8494, 1573, 1408
Criterion for observed reflections	$I > 2\sigma(I)$	$I > 2\sigma(I)$	$I > 2\sigma(I)$	$I > 2\sigma(I)$	$I > 2\sigma(I)$	$I > 2\sigma(I)$
R_{int}	0.071	0.035	0.140	0.059	0.101	0.046
θ_{max} (°)	27.49	27.4	27.46	27.44	27.47	27.47
Range of h, k, l	$-12 \rightarrow h \rightarrow 12$ $-10 \rightarrow k \rightarrow 11$ $-16 \rightarrow l \rightarrow 16$	$-26 \rightarrow h \rightarrow 26$ $-4 \rightarrow k \rightarrow 6$ $-20 \rightarrow l \rightarrow 21$	$-28 \rightarrow h \rightarrow 26$ $-5 \rightarrow k \rightarrow 5$ $-22 \rightarrow l \rightarrow 22$	$-14 \rightarrow h \rightarrow 14$ $-6 \rightarrow k \rightarrow 7$ $-18 \rightarrow l \rightarrow 18$	$-8 \rightarrow h \rightarrow 8$ $-20 \rightarrow k \rightarrow 20$ $-14 \rightarrow l \rightarrow 14$	$-30 \rightarrow h \rightarrow 31$ $-4 \rightarrow k \rightarrow 4$ $-16 \rightarrow l \rightarrow 19$
Intensity decay (%)	0	0	0	0	0	0
Refinement						
Refinement on	F^2	F^2	F^2	F^2	F^2	F^2
$R[F^2>2\sigma(F^2)]$, $wR(F^2)$, S	0.044, 0.124, 1.05	0.044, 0.123, 1.06	0.069, 0.193, 1.05	0.069, 0.162, 1.21	0.057, 0.164, 1.04	0.032, 0.082, 1.03
No. of reflections and parameters used in refinement	2430, 147	1653, 101	1782, 106	2003, 139	2583, 199	1573, 182
H-atom treatment	H-atom parameters constrained	H-atom parameters constrained	H-atom parameters constrained	H-atom parameters constrained	H-atom parameters constrained	H-atom parameters constrained
Weighting scheme	$w = 1/[\sigma^2(F_o^2) + (0.0622P)^2 + 0.2854P]$ where $P = (F_o^2 + 2F_c^2)/3$	$w = 1/[\sigma^2(F_o^2) + (0.0482P)^2 + 0.3635P]$ where $P = (F_o^2 + 2F_c^2)/3$	$w = 1/[\sigma^2(F_o^2) + (0.1093P)^2]$ where $P = (F_o^2 + 2F_c^2)/3$	$w = 1/[\sigma^2(F_o^2)P)^2 + 1.1216P]$ where $P = (F_o^2 + 2F_c^2)/3$	$w = 1/[\sigma^2(F_o^2) + (0.0644P)^2 + 0.4931P]$ where $P = (F_o^2 + 2F_c^2)/3$	$w = 1/[\sigma^2(F_o^2) + (0.0458P)^2 + 0.1414P]$ where $P = (F_o^2 + 2F_c^2)/3$
$(\Delta/\sigma)_{max}$	<0.001	<0.001	<0.001	<0.001	<0.001	<0.001
$\Delta\rho_{max}, \Delta\rho_{min}$ (e Å^{-3})	0.26, −0.31	0.27, −0.23	0.27, −0.31	0.27, −0.30	0.28, −0.25	0.18, −0.15
Extinction method	None	None	*SHELXL*	*SHELXL*	*SHELXL*	*SHELXL*
Extinction coefficient	–	–	0.020 (6)	0.024 (4)	0.046 (7)	0.018 (4)

Computer programs used: *PRPKAPPA* (Ferguson, 1999), Kappa-CCD (Nonius, 1997), *DENZO-SMN* (Otwinowski & Minor, 1997), *SHELXL*97 (Sheldrick, 1997*a*), *SHELXS*97 (Sheldrick, 1997*b*). † See Scheme I for identifcation of *A*–*J*.

HMTA yielded predominantly ammonium hydrogenfumarate, $[(NH_4)^+]\cdot[(C_4H_3O_4)^-]$. This product was contaminated by a very small quantity of material that was shown by the structure analysis to be a 1:1 adduct that contains HMTA and, most unexpectedly, an approximately 3:1 mixture of fumaric and succinic acids, in which the amine is monoprotonated $[\{(C_6H_{12}N_4)H\}^+]$ and the acid components form the mono-anions $[(C_4H_3O_4)^-]$ and $[(C_4H_5O_4)^-]$.

Table 2
Hydrogen bond parameters (Å, °).

D—H···A	H···A	D···A	D—H···A	
(1)	O3—H3···O2	1.61	2.453 (2)	178
	N11—H11···O1	1.76	2.637 (2)	173
	C12—H12···O1^{i}	2.34	3.246 (2)	158
	C13—H13···O4^{ii}	2.40	3.272 (2)	153
	C15—H15···O3^{iii}	2.47	3.274 (2)	143
(2)	O3—H3···O2	1.62	2.463 (2)	176
	N11—H11···O1	1.75	2.627 (2)	171
	C13—H13···O4^{iv}	2.37	3.315 (2)	175
	C15—H15···O4^{v}	2.38	3.176 (2)	142
	C16—H16···O1^{vi}	2.28	3.223 (2)	170
(3)	O11—H11···O21^{vii}	1.66	2.495 (2)	175
	N1—H1···O21	1.87	2.751 (2)	174
	N11—H11*A*···O12^{viii}	2.25	2.869 (2)	128†
	N11—H11*A*···N21	1.98	2.651 (2)	132†
	C16—H16···O22^{ix}	2.28	3.052 (2)	138‡
	C16—H16···O12^{viii}	2.51	3.013 (2)	113‡
(4)	O1—H1···O4^{x}	1.71	2.551 (2)	174
	N1—H1*A*···O3	1.74	2.651 (2)	166
(5)	O1—H1···N11	1.76	2.603 (2)	179
	C15—H15···O2^{xi}	2.43	3.301 (2)	153
(6)	N1—H1···O1	1.64	2.559 (2)	171
	O1—H1*A*···N1	1.72	2.559 (2)	177
	N2—H2···O3^{xii}	1.66	2.592 (2)	178
	C23—H23*A*···O4^{viii}	2.33	3.144 (2)	139
(7)	O1—H1···N11	1.73	2.567 (2)	172
	C16—H16···O1^{iv}	2.55	3.217 (2)	128
(8)	O1—H1···N11	1.76	2.595 (2)	172
	C16—H16···O1^{xiii}	2.57	3.232 (2)	127
(9)	O2—H2···O3	1.64	2.477 (3)	175
	O4—H4···O4^{xiv}	1.63	2.451 (3)	164
	N11—H11···N12^{xv}	1.82	2.548 (4)	137
	N1—H1···O1	1.83	2.679 (5)	163
	N11—H11···O1	2.70	3.272 (4)	123
	C13—H13···O2^{xv}	2.54	3.454 (4)	162
	C15—H15···O4^{xvi}	2.47	3.128 (4)	127
(10)	O4—H4···O1^{xvii}	1.67	2.507 (4)	173
	O44—H44···O1^{xvii}	1.62	2.446 (11)	165
	O4—H4···O41^{xvii}	1.75	2.560 (11)	160
	O44—H44···O41^{xvii}	1.74	2.578 (14)	176
	N1—H1···O1	1.99	2.868 (4)	156
	N1—H1···O41	2.15	2.965 (11)	146
	C12—H12*A*···O4^{xviii}	2.52	3.360 (5)	143
	C34—H34*A*···O3^{xix}	2.45	3.371 (4)	155
(11)	O1—H1···N11	1.86	2.693 (2)	173
	O3—H3···N21^{xx}	1.82	2.654 (2)	172
	C14—H14···O4^{xxi}	2.43	3.372 (3)	173
	C16—H16···O2	2.45	3.171 (3)	132

Symmetry codes: (i) $3-x, -y, 1-z$; (ii) $-1+x, 1+y, 1+z$; (iii) $2-x, -y, -z$; (iv) $\frac{1}{2}-x, \frac{1}{2}+y, \frac{1}{2}-z$; (v) $\frac{1}{2}+x, \frac{1}{2}+y, z$; (vi) $1-x, y, \frac{3}{2}-z$; (vii) $1+x, y, z$; (viii) $1-x, -y, 1-z$; (ix) $x, y, 1+z$; (x) $x, 1-y, -\frac{1}{2}+z$; (xi) $1-x, 2-y, 1-z$; (xii) $1+x, \frac{1}{2}-y, -\frac{1}{2}+z$; (xiii) $\frac{3}{2}-x, \frac{1}{2}+y, \frac{3}{2}-z$; (xiv) $-x, 4-y, 1-z$; (xv) $1-x, 1-y, 1-z$; (xvi) $\frac{1}{2}-x, -\frac{3}{2}+y, \frac{3}{2}-z$; (xvii) $-1+x, y, z$; (xviii) $1-x, \frac{1}{2}+y, \frac{1}{2}-z$; (xix) $2-x, 1-y, 1-z$; (xx) $\frac{1}{2}+x, 2-y, z$; (xxi) $\frac{1}{2}-x, -1+y, \frac{1}{2}+z$. † Three-centre N—H···(N,O) hydrogen bond: sum of angles at H11*A*, 359°. ‡ Three-centre C—H···(O)$_2$ hydrogen bond: sum of angles at H16, 354°.

Note that (2) and (5), the 1:2 and 1:1 adducts that are formed by 4,4′-bipyridyl with maleic and fumaric acids, respectively, crystallize in space groups $C2/c$ and $P\bar{1}$, while the corresponding pair of adducts that are formed by 1,2-bis(4-pyridyl)ethane, (1) and (7), reverse this pattern by crystallizing in $P\bar{1}$ and $C2/c$, respectively. Similarly, the 1:2 and 1:1 adducts that are formed by DABCO with fumaric acid, (4) and (6), crystallize in space groups $C2/c$ and $P2_1/c$, respectively, while the 1:2 adduct that is formed by DABCO with maleic acid crystallizes in space group $Cmc2_1$ (Sun & Jin, 2002). Finally, the adducts that are formed by 2,2′-dipyridylamine with maleic and fumaric acids, (9) and (3), crystallize in $P2_1/n$ and $P\bar{1}$, respectively. Note also the close similarity between the cell dimensions of (7) and (8), which are both in $C2/c$ (Table 1); despite this similarity, the supramolecular structures exhibit very different chain directions (§3.3.5) because of the different selection of special positions that are occupied in the two cases. We note also the very short a axis in (5) and the very short b axis in (11); in (11) the result is a unit cell of markedly tabular shape.

The maleic acid adducts (1) and (2) have constitutions of general type $[\{(\text{diamine})H_2\}^{2+}]\cdot[(C_4H_3O_4)^-]_2$, where the monoanion contains a short and nearly linear, but asymmetric, O—H···O hydrogen bond. The fumaric acid adduct (4) likewise has the constitution $[\{(\text{diamine})H_2\}^{2+}]\cdot[(C_4H_3O_4)^-]_2$. The fumaric acid adducts (5), (7), (8) and (11) all have constitutions of type [diamine]·[$C_4H_4O_4$] in which both components are neutral, while (10) contains simple monocations and monoanions. A fumarate monoanion is present in (3), $[\{(C_{10}H_9N_3)H\}^+]\cdot[(C_4H_3O_4)^-]$, where the cation contains an intramolecular N—H···N hydrogen bond, but in (9) only partial H-atom transfer has occurred to give $[\{(C_{10}H_9N_3)H\}^+]\cdot[(C_4H_{3.5}O_4)^{-0.5}]_2$. The constitution of (6) is more complex: one carboxyl H atom has been fully transferred from O to N, and the other is only partially transferred, such that (6) must be represented thus: $[\{(C_6H_{12}N_2)H_{1.57}\}^{+1.57}]\cdot[(C_4H_{2.43}O_4)^{-1.57}]$.

3.2. Molecular conformations and dimensions

In (5), the two rings of the 4,4′-bipyridyl component are constrained by the centre of inversion to be parallel: where no such symmetry constraint is present, as in (2) and (11), the two rings of the 4,4′- and 2,2′-bipyridyl units exhibit significant twists away from coplanarity (Table 3). However, in each of (1), (7) and (8) the pyridyl rings are almost orthogonal to the planar central spacer units. The differences in molecular conformation of the pyridines may well be a result of the different patterns of the C—H···O hydrogen bonds associated with each compound. Again, the near planarity of the cation in (3) is almost certainly associated with its intramolecular N—H···N hydrogen bond. Possibly the most striking feature of the DABCO units in (4) and (6) is the widely different degree of twist away from the idealized D_{3h} symmetry: the mean N—C—C—N torsional angle is almost an order of magnitude greater in (4) than in (6). The acid components – whether neutral as in (5), (7), (8) and (11), or monoanions as in (1)–(4) and (10), or of fractional charge as in (6) and (9) – are nearly all very close to planarity. The minor succinate component $(C_4H_5O_4)^-$ in (10) has an unusual eclipsed anticlinal conformation with a torsional angle C41—C42—C43—C44 of 121.7 (9)°.

In general the molecular dimensions show no unusual features, but the dimensions of the cation of (10) are worthy of comment. In this cation $[\{(C_6H_{12}N_4)H\}^+]$ the C—N distances fall into three clear ranges (Table 4): those involving the protonated N1 have mean value 1.512 (3); those sharing a C atom with a member of the first group have mean value

1.443 (3); and the remaining six C—N distances, those most remote from the site of protonation, have mean value 1.469 (3). It is notable that there are no overlaps between the ranges that are spanned by the three types of bond. While the mean length of the C—N bonds of sixfold multiplicity is entirely as expected for a tertiary aliphatic amine [mean of 1042 values, 1.469 (Allen *et al.*, 1987)], the bonds to N1 are very much longer and the bonds β to N1 are much shorter. It is of interest to consider the pattern of the C—N bond lengths in terms of the likely mechanism for the early steps in the acid-promoted decomposition of HMTA (Scheme II), where a

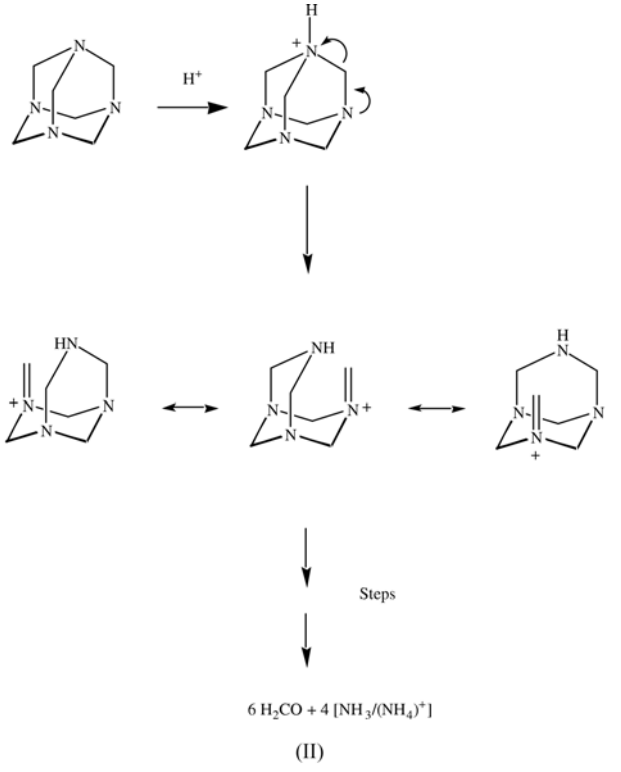

(II)

C—N bond adjacent to the protonated N is cleaved while the corresponding β bond is converted to the C=N double bond of an iminium cation. The observed cation structure in (10) suggests that this cation is well advanced along the reaction coordinate from the T_d structure of neutral tricyclic HMTA to the bicyclic iminium intermediate (Scheme II).

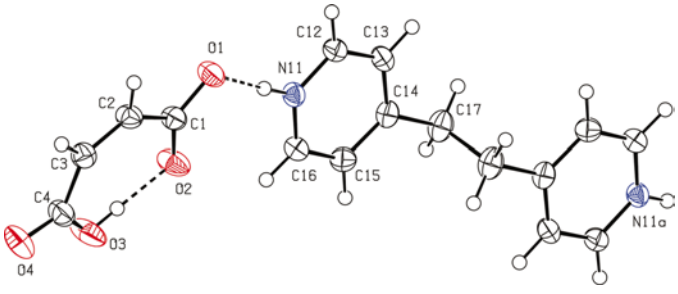

Figure 1
The components of (1) and the atom-labelling scheme. Displacement ellipsoids are drawn at the 50% probability level. The atom marked '*a*' is at the symmetry position $(1-x, 1-y, 1-z)$.

In the reactions conducted here, which gave rise to mixtures of ammonium hydrogenfumarate and (10), the deficiency of acid required to protonate all of the ammonia that arises from the decomposition of the HTMA means that the pH of the reaction solution will tend to rise as the reaction proceeds. Since methanol can act as a reducing agent in basic media, this rise in pH may account for the reduction of some of the fumaric acid to succinic acid: however, no specific investigation of that reduction was conducted during this study.

3.3. Description of the supramolecular structures

In the maleate salts (1) and (2), the hard N—H···O hydrogen bonds (Table 2) link the components into finite three-ion aggregates, anion—cation—anion, and these aggregates are further linked by soft C—H···O hydrogen bonds to give a two-dimensional supramolecular structure in the case of (1) and a three-dimensional supramolecular structure in the case of (2). By contrast, in the maleate salt (9), the hard hydrogen bonds generate chains that contain alternating cations and anions; these chains are further linked by C—H···O hydrogen bonds to form a three-dimensional framework.

The dominant structural characteristic of the fumaric acid adducts is the formation of chains by means of hard hydrogen bonds. As in the maleic acid systems, these chains may be subject to further linking by means of C—H···O hydrogen bonds. In (3) and (4) the chain formation involves only fumarate monoanions $(C_4H_3O_4)^-$, and pairs of chains are linked by the cations to form isolated molecular ladders in

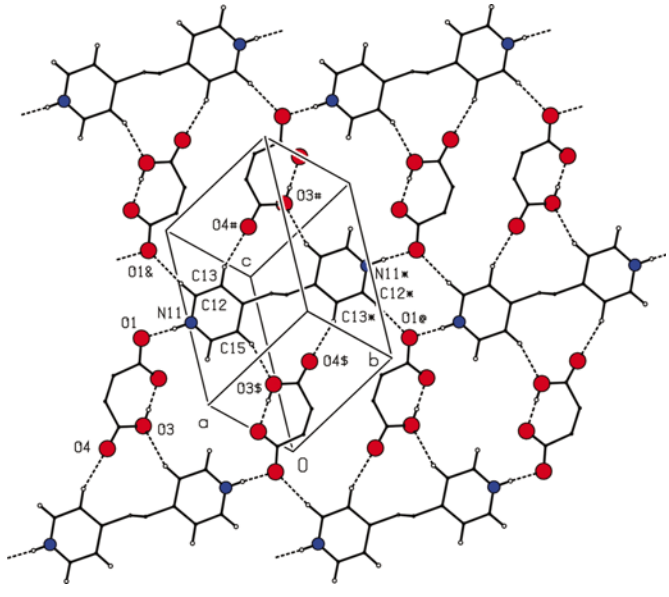

Figure 2
Part of the crystal structure of (1), which shows the formation of a sheet containing four types of ring. For the sake of clarity, H atoms bonded to C2, C3 and C17 are omitted. The atoms marked with an asterisk (*), hash (#), dollar sign ($), ampersand (&) or at sign (@) are at the symmetry positions $(1-x, 1-y, 1-z)$, $(-1+x, 1+y, 1+z)$, $(2-x, -y, -z)$, $(3-x, -y, 1-z)$ and $(-2+x, 1+y, z)$, respectively.

Table 3
Selected dihedral and torsional angles in diamine components (°).

(*a*) Amine components				
(1)	(N11—C16)^(C14,C17,C17^{i},C14^{i})	81.6 (2)		
(2)	(N11—C16)^(N11^{ii}—C16^{ii})	22.2 (2)		
(3)	N11—C12—N1—C22	−3.7 (3)	N21—C22—N1—C12	−5.5 (3)
(4)	N1—C6—C6^{iii}—N1^{iii}	−19.7 (2)	N1—C5—C7^{iii}—N1^{iii}	−21.2 (3)
(6)	N1—C11—C21—N2	−2.1 (2)	N1—C12—C22—N2	−2.7 (2)
	N1—C13—C23—N2	−1.1 (2)		
(7)	(N11—C16)^(C14,C17,C17^{i},C14^{i})	87.2 (2)		
(8)	C13—C14—C17—C18	92.2 (2)	C14—C17—C18—C17^{iii}	−179.4 (2)
(9)	N12—C11—N1—C12^{i}	2.8 (7)	N11—C12—N1^{i}—C11^{i}	2.7 (7)
(11)	(N11—C16)^(N21—C26)	37.2 (2)		
(*b*) Acid components				
(1)	O1—C1—C2—C3	178.2 (2)	O4—C4—C3—C2	178.0 (2)
(2)	O1—C1—C2—C3	−178.2 (2)	O4—C4—C3—C2	−178.3 (2)
(3)	O11—C1—C2—C3	175.6 (2)	O21—C4—C3—C2	−169.9 (2)
(4)	O1—C1—C2—C3	179.5 (2)	O4—C4—C3—C2	−168.1 (2)
(5)	O1—C1—C2—C2^{iv}	−4.4 (2)		
(6)	O1—C1—C2—C3	173.0 (2)	O4—C4—C3—C2	166.7 (2)
(7)	O1—C1—C2—C2^{v}	2.6 (3)		
(8)	O1—C1—C2—C2^{vi}	−2.3 (4)		
(9)	O1—C1—C2—C3	174.7 (3)	O4—C4—C3—C2	−176.6 (3)
(10)	O1—C1—C2—C3	177.6 (4)	O4—C4—C3—C2	175.8 (4)
(11)	O1—C1—C2—C3	−176.6 (2)	O4—C4—C3—C2	−4.1 (2)

Symmetry codes: (i) $1-x, 1-y, 1-z$; (ii) $1-x, y, \frac{1}{2}-z$; (iii) $1-x, y, \frac{3}{2}-z$; (iv) $-1-x, 2-y, -z$; (v) $\frac{1}{2}-x, -\frac{3}{2}-y, -z$; (vi) $\frac{3}{2}-x, \frac{1}{2}-y, 1-z$.

Table 4
Bond lengths in the cation of (10) (Å).

N1—C12	1.513 (3)	N2—C12	1.447 (3)
N1—C13	1.509 (3)	N3—C13	1.443 (3)
N1—C14	1.515 (3)	N4—C14	1.439 (3)
N2—C23	1.464 (3)	N2—C24	1.467 (3)
N3—C23	1.471 (3)	N3—C34	1.467 (3)
N4—C24	1.480 (3)	N4—C34	1.465 (3)

each case. Of the remaining fumaric acid derivatives, in (5), (6), (7), (8) and (11) the chains comprise alternating diamine and acid units, regardless of the extent (if any) of H-atom transfer between acid and base. These chains are linked by C—H···O hydrogen bonds to form sheets in (5) and (6), to form single three-dimensional frameworks in (7) and (8), and to form a double framework in (11). The chain formation in (10) depends solely on the anions, but again the C—H···O hydrogen bonds link the anions into a single three-dimensional framework. These general patterns provide a convenient basis on which to consider in detail the supramolecular structures adopted by each compound.

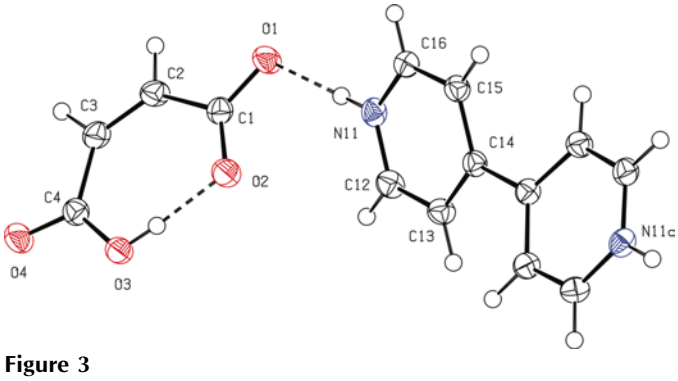

Figure 3
The components of (2) and the atom-labelling scheme. Displacement ellipsoids are drawn at the 50% probability level. The atom marked '*a*' is at the symmetry position $(1-x, y, \frac{1}{2}-z)$.

3.3.1. Three-ion aggregates are linked by C—H···O hydrogen bonds into sheets. *Compound (1)*. In this salt (Fig. 1) the diprotonated diamine $[\{(C_{12}H_{12}N_2)H_2\}^{2+}]$ lies across a centre of inversion, which is chosen for the sake of convenience as that at $(\frac{1}{2}, \frac{1}{2}, \frac{1}{2})$. Within the anion there is a short but asymmetric O—H···O hydrogen bond, and the ions are linked by the N—H···O hydrogen bond into finite three-ion aggregates that are themselves linked into a continuous sheet by three different C—H···O hydrogen bonds.

Atom C12 at (x, y, z) acts as hydrogen-bond donor to O1 in the anion at $(3-x, -y, 1-z)$, while C12 at $(3-x, -y, 1-z)$ in turn acts as donor to O1 at (x, y, z), so that an $R_4^2(10)$ ring centred at $(\frac{3}{2}, 0, \frac{1}{2})$ is generated. Propagation of this interaction by inversion thus leads to the formation of a $C_2^1(12)[R_4^2(10)]$ chain of rings (Bernstein *et al.*, 1995) that runs parallel to the $[\bar{2}10]$ direction (Fig. 2). In the three-ion aggregate centred at $(\frac{1}{2}, \frac{1}{2}, \frac{1}{2})$, atoms C15 at (x, y, z) and C13 at $(1-x, 1-y, 1-z)$ act as hydrogen-bond donors, respectively, to O3 and O4 in the anion at $(2-x, -y, -z)$, which lies in the three-ion aggregate that is centred at $(\frac{3}{2}, -\frac{1}{2}, -\frac{1}{2})$. The symmetry-related C atoms in the $(\frac{1}{2}, \frac{1}{2}, \frac{1}{2})$ aggregate donate hydrogen bonds to the anion at $(-1+x, 1+y, 1+z)$, which is part of the three-ion aggregate that is centred at $(-\frac{1}{2}, \frac{3}{2}, \frac{3}{2})$. In this manner a perforated ribbon, or chain of fused rings, is generated parallel to $[\bar{1}11]$; in this chain, centrosymmetric $R_6^6(20)$ rings alternate with centrosymmetrically related pairs of $R_2^2(11)$ rings. The combination of the $[\bar{1}11]$ ribbons with the $[\bar{2}10]$ chain of rings generates a sheet that contains, in addition to the ring within the anion, four types of ring, three of them centrosymmetric. In these four types of ring the linking of the $[\bar{1}11]$ ribbons also generates $R_4^4(20)$ rings (Fig. 2).

3.3.2. Three-ion aggregates are linked by C—H···O hydrogen bonds into frameworks. *Compound (2)*. The cation in (2) (Fig. 3) lies across a twofold rotation axis in space group *C*2/*c*. This axis is chosen as that along $(\frac{1}{2}, y, \frac{1}{4})$, where the centroid of the cation has $y \simeq 0.28$. The anion contains a short but asymmetric O—H···O hydrogen bond, and the ions are linked, as in (1), into three-ion aggregates by means of a single N—H···O hydrogen bond (Table 2).

The three-ion aggregates are linked by three C—H···O hydrogen bonds into a continuous three-dimensional framework: each cation thus contains the donor in six such interactions. In the reference cation across the $(\frac{1}{2}, y, \frac{1}{4})$ rotation axis, atoms C15 at (x, y, z) and C13 at $(1-x, y, \frac{1}{2}-z)$ both act as

hydrogen-bond donors to atom O4 in the anion at $(\frac{1}{2}+x, \frac{1}{2}+y, z)$, while C15 at $(\frac{1}{2}+x, \frac{1}{2}+y, z)$ and C13 at $(\frac{3}{2}-x, \frac{1}{2}+y, \frac{1}{2}-z)$, which lie in a cation across the rotation axis along $(1, y, \frac{1}{4})$, both act as donors to O4 at $(1+x, 1+y, z)$, so generating by means of the *C*-centring translation a $C_2^2(11)C_2^2(14)[R_2^1(7)]$ chain of rings that runs parallel to the [110] direction (Fig. 4). The action of the twofold rotation axes generates a similar chain of rings parallel to $[1\bar{1}0]$, and the combination of these two chains generates a (001) sheet.

The (001) sheets that are related by translation are linked by the final C—H···O hydrogen bond. C16 at (x, y, z), which is part of the cation across $(\frac{1}{2}, y, \frac{1}{4})$, acts as hydrogen-bond donor to O1 in the anion at $(1-x, y, \frac{3}{2}-z)$. This anion forms part of the three-ion aggregate that lies across the rotation axis $(\frac{1}{2}, y, \frac{5}{4})$. Propagation of this hydrogen bond by the twofold axes generates a $C_2^2(10)[R_4^2(10)]$ chain of rings that is parallel to [001] (Fig. 5). This chain links successive (001) sheets into a continuous framework. This framework, however, encompasses only half the contents of the unit cell, and there is a second framework that is related to the first by inversion. These two frameworks are continuously interwoven. No hydrogen bonds link the two frameworks, but they are linked by weak aromatic $\pi\cdots\pi$ stacking interactions. The parallel pyridinium rings at (x, y, z) and $(1-x, 1-y, 1-z)$, which lie in different frameworks, have an interplanar spacing of 3.378 (2) and a centroid separation of 3.758 (2), which correspond to a centroid offset of 1.647 (2) (Fig. 6).

3.3.3. Anion chains are linked into molecular ladders. *Compound (3)*. Compound (3) (Fig. 7) is a salt $[\{(C_{10}H_9N_3)H\}^+]\cdot[(C_4H_3O_4)^-]$ in which the conformation of the cation is apparently controlled by the formation of an intramolecular N—H···N hydrogen bond, which generates an *S*(6) motif. It is possible to identify a simple anion substructure in the form of a *C*(7) chain that is generated by translation. The carboxyl O11 in the anion at (x, y, z) acts as hydrogen-bond donor to the carboxylate O21 in the anion at $(1+x, y, z)$. Pairs of antiparallel chains, where the chains within a pair are related to one another by inversion centres, are linked by the cations into molecular ladders in which the anion chains play the role of the uprights and the cations act as the rungs of the ladder.

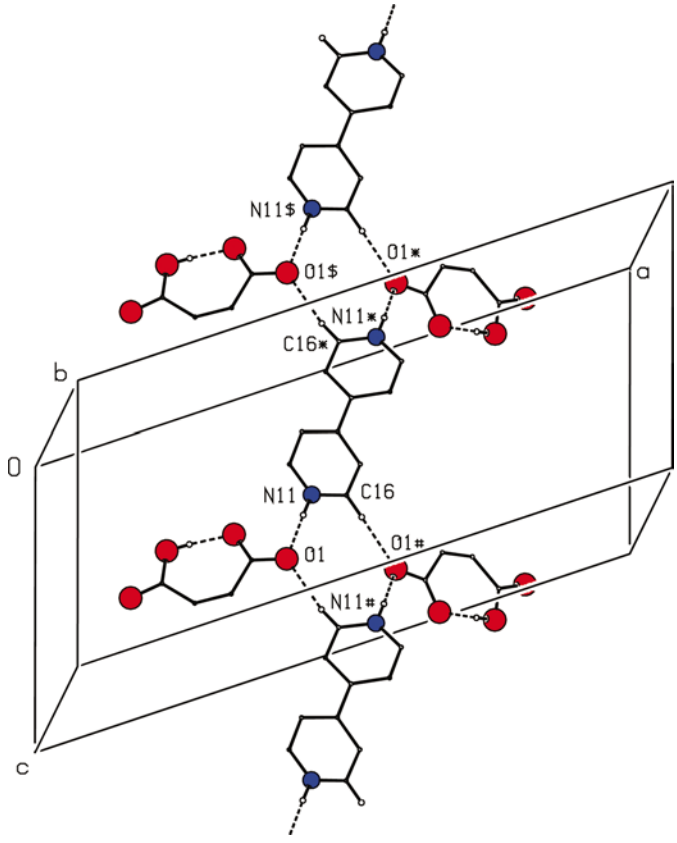

Figure 5
Part of the crystal structure of (2), which shows the formation of a chain of rings along [001]. For the sake of clarity, the only H atoms bonded to C shown are those involved in the hydrogen-bond motif depicted. The atoms marked with an asterisk (*), hash (#) or dollar sign ($) are at the symmetry positions $(1-x, y, \frac{1}{2}-z)$, $(1-x, y, \frac{3}{2}-z)$ and $(x, y, -1+z)$, respectively.

In the cation at (x, y, z), the amino N1 acts as hydrogen-bond donor to the carboxylate O21 in the anion at (x, y, z). The pyridinium N11, as well as forming the intramolecular hydrogen bond, also acts as donor to the carboxylate O12 in the anion at $(1-x, -y, 1-z)$, in an effectively planar N—H···(N,O) system. In this way a molecular ladder is generated that runs along the line $(x, 0, \frac{1}{2})$: between the rungs there are $R_4^4(22)$ rings centred at $(n+\frac{1}{2}, 0, \frac{1}{2})$ (n = zero or integer) and $R_6^4(20)$ rings centred at $(n, 0, \frac{1}{2})$ (n = zero or integer) (Fig. 8).

The [100] molecular ladders are linked into (010) sheets by a single, rather short, C—H···O hydrogen bond (Table 2). Atom C16 is adjacent to the protonated N11: C16 in the cation at (x, y, z) acts as hydrogen-bond donor to the carboxylate O22 in the anion at $(x, y, 1+z)$, so generating by transla-

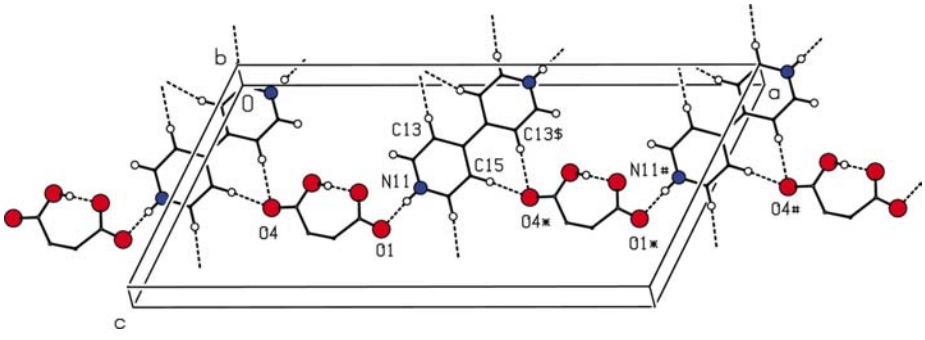

Figure 4
Part of the crystal structure of (2), which shows the formation of a chain of rings along [110]. For the sake of clarity H atoms bonded to C2 and C3 are omitted. The atoms marked with an asterisk (*), hash (#) or dollar sign ($) are at the symmetry positions $(\frac{1}{2}+x, \frac{1}{2}+y, z)$, $(1+x, 1+y, z)$ and $(1-x, y, \frac{1}{2}-z)$, respectively.

tion a $C_2^2(9)$ chain along [001] (Fig. 9). At the same time, C16 at (x, y, z) also acts, more weakly, as donor to O12 in the anion at ($1-x$, $-y$, $1-z$), so forming the rather uncommon three-centre C—H···$(O)_2$ system, the longer component of which serves to reinforce the formation of the ladder.

Compound (4). The 1:2 adduct, (4) (Fig. 10), that is formed between DABCO and fumaric acid is a salt, $[\{(C_6H_{12}N_2)H_2\}^{2+}]\cdot[(C_4H_3O_4)^-]_2$, in which the dication lies across a twofold rotation axis in space group $C2/c$, while the anion lies in a general position.

As in (3), it is possible to identify a simple substructure that consists of a $C(7)$ chain formed by the anions alone, but in (4) this chain is generated by a glide plane, whereas the corresponding chain in (3) is generated by translation. In (4), the carboxyl O1 in the anion at (x, y, z) acts as hydrogen-bond donor to the carboxylate O4 in the anion at (x, $1-y$, $-\frac{1}{2}+z$), while O1 at (x, $1-y$, $-\frac{1}{2}+z$) in turn acts as donor to O4 at (x, y, $-1+z$). Thus a $C(7)$ chain, which runs parallel to the [001] direction and lies along the approximate line ($\frac{1}{5}$, $\frac{1}{2}$, z) (Fig. 11), is generated by the c-glide plane at $y=\frac{1}{2}$. There are four such chains passing through each unit cell and they are linked in pairs by the cations to form molecular ladders.

In the cation, which lies across the twofold axis along ($\frac{1}{2}$, y, $\frac{3}{4}$), the atoms N1 at (x, y, z) and ($1-x$, y, $\frac{3}{2}-z$) act as hydrogen-bond donors, respectively, to the carboxylate O3 acceptors in the anions at (x, y, z) and ($1-x$, y, $\frac{3}{2}-z$): the anion at ($1-x$, y, $\frac{3}{2}-z$) lies in a $C(7)$ chain, which is anti-parallel to the reference chain and which lies along the approximate line ($\frac{4}{5}$, $\frac{1}{2}$, $-z$). In the resulting molecular ladder, in which the $C(7)$ anion chains act as the uprights and the cations as the rungs, there are $R_6^6(32)$ rings between adjacent rungs (Fig. 11). Two molecular ladders run through each unit cell, in the domains $0.18 < y < 0.76$ and $0.68 < y < 1.26$, but

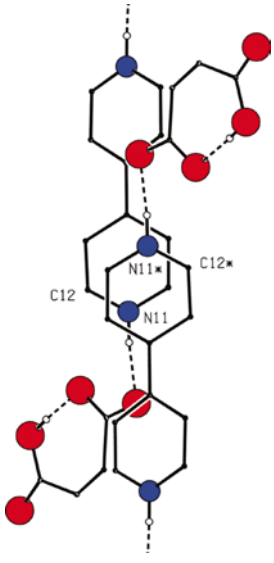

Figure 6
Part of the crystal structure of (2), which shows the $\pi\cdots\pi$ stacking interaction that links the two frameworks. For the sake of clarity, H atoms bonded to C are omitted. The atoms marked with an asterisk (*) are at the symmetry position ($1-x$, $1-y$, $1-z$).

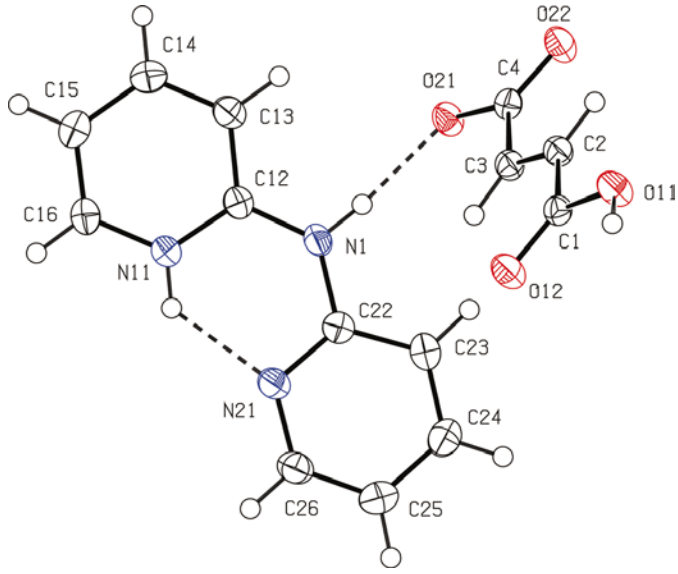

Figure 7
The components of (3) and the atom-labelling scheme. Displacement ellipsoids are drawn at the 50% probability level.

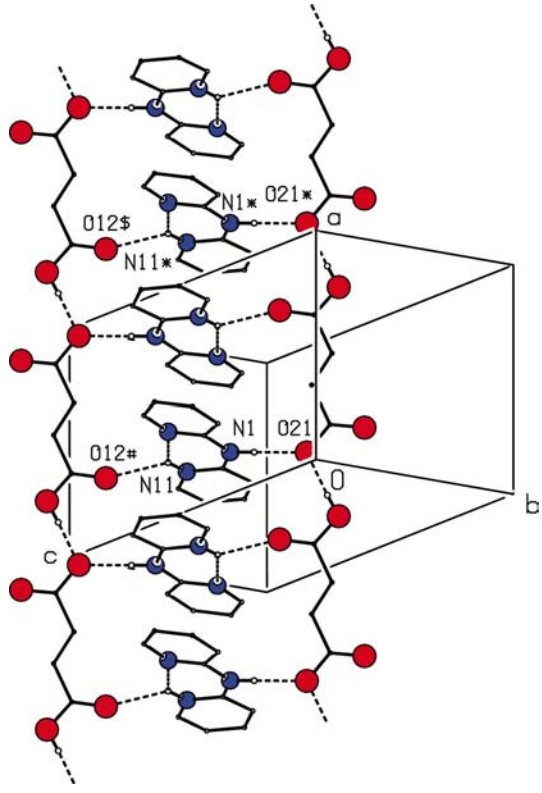

Figure 8
Part of the crystal structure of (3), which shows the formation of a molecular ladder along [100]. For the sake of clarity, H atoms bonded to C are omitted. The atoms marked with an asterisk (*), hash (#) or dollar sign ($) are at the symmetry positions ($1+x$, y, z), ($1-x$, $-y$, $1-z$) and ($2-x$, $-y$, $1-z$), respectively.

there are no direction-specific interactions between adjacent ladders.

3.3.4. Chains are linked by C—H···O hydrogen bonds into sheets. *Compound (5)*. In the 1:1 adduct, (5), that is formed between 4,4′-bipyridyl and fumaric acid both components are neutral with no evidence for any transfer of H atoms from O to N atoms. Both components lie across centres of inversion and they are linked into chains by a single O—H···N hydrogen bond. With the diamine located across the centre of inversion at $(\frac{1}{2}, \frac{1}{2}, \frac{1}{2})$, the selected asymmetric unit (Fig. 12) requires the acid molecule to be located across the centre of inversion at $(-\frac{1}{2}, 1, 0)$. Propagation of the N—H···O hydrogen bond by inversion (Table 2) thus generates a $C_2^2(16)$ chain that runs parallel to the $[2\bar{1}1]$ direction (Fig. 13).

The chains thus generated are linked by a single C—H···O hydrogen bond (Table 2) to form sheets. Atom C15 at (x, y, z), which is part of the diamine centred at $(\frac{1}{2}, \frac{1}{2}, \frac{1}{2})$, acts as hydrogen-bond donor to O2 at $(1 - x, 2 - y, 1 - z)$, which is part of the acid lying across the centre of inversion at $(\frac{3}{2}, 1, 1)$. Propagation by inversion of this hydrogen bond generates a $C_2^2(12)$ chain that runs parallel to the [211] direction, and the

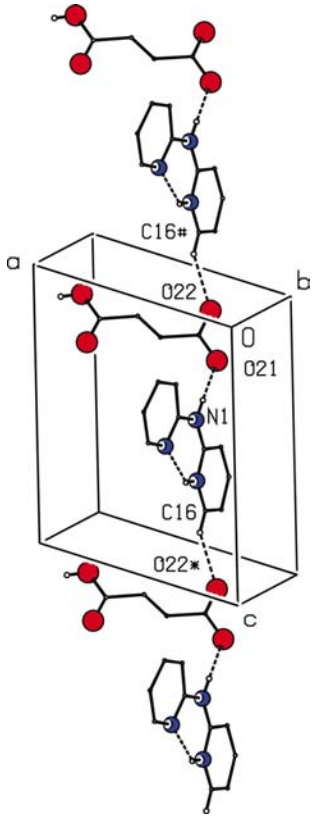

Figure 9
Part of the crystal structure of (3), which shows the $C_2^2(9)$ chain along [001] that links the [100] ladders into a (010) sheet. For the sake of clarity, the only H atom bonded to C shown is that involved in the chain formation. The atoms marked with an asterisk (*) or a hash (#) are at the symmetry positions $(x, y, 1 + z)$ and $(x, y, -1 + z)$, respectively.

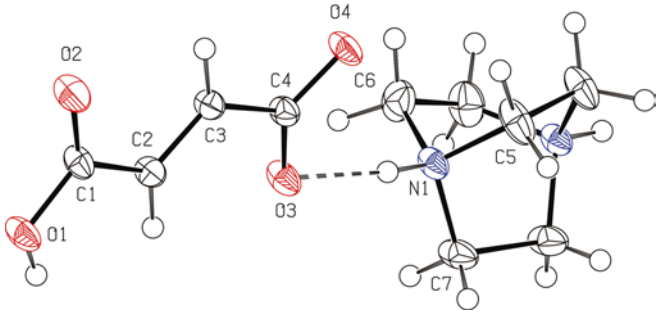

Figure 10
The components of (4) and the atom-labelling scheme. Displacement ellipsoids are drawn at the 50% probability level: the cation lies across a twofold rotation axis.

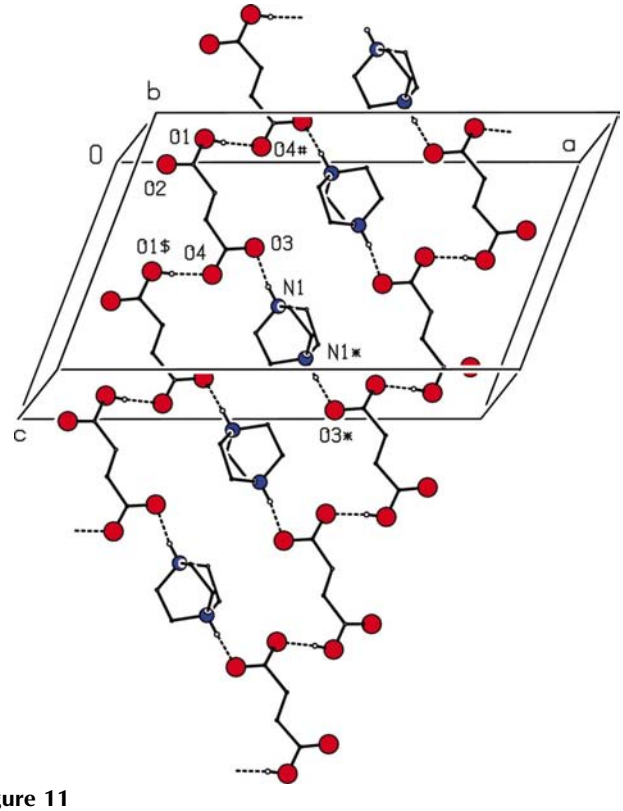

Figure 11
Part of the crystal structure of (4), which shows the formation of a molecular ladder along [001]. For the sake of clarity, H atoms bonded to C are omitted. The atoms marked with an asterisk (*), hash (#) or dollar sign ($) are at the symmetry positions $(1 - x, y, \frac{3}{2} - z)$, $(x, 1 - y, -\frac{1}{2} + z)$ and $(x, 1 - y, \frac{1}{2} + z)$, respectively.

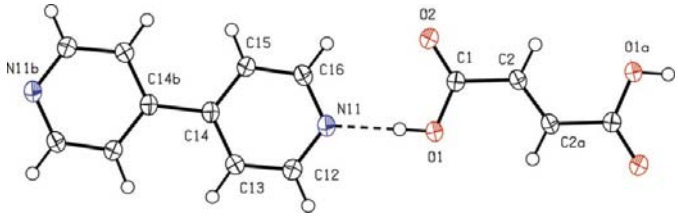

Figure 12
The components of (5) and the atom-labelling scheme. Displacement ellipsoids are drawn at the 30% probability level. The atoms marked '*a*' or '*b*' are at the symmetry positions $(-1 - x, 2 - y, -z)$ and $(1 - x, 1 - y, 1 - z)$, respectively.

combination of the [211] and [2$\bar{1}$1] chains generates a (10$\bar{2}$) sheet built from $R_4^4(16)$ and $R_4^4(28)$ rings, both centrosymmetric, that alternate in checkerboard fashion (Fig. 13). There are neither C—H···π(arene) hydrogen bonds nor aromatic $\pi\cdots\pi$ stacking interactions in the structure of (5), thus the supramolecular structure defined by the direction-specific interactions is two dimensional.

Compound (6). In the 1:1 adduct, (6), that is formed between DABCO and fumaric acid, one acidic H atom has been transferred completely from O to N, while the other acidic H atom has been transferred only partially. Within the asymmetric unit (Fig. 14) there are two H-atom sites between N1 and O1. The site nearer to N1 (labelled H1) has occupancy 0.57 (3) and the site nearer to O1 (labelled H1*A*) has occupancy 0.43 (3), so that a disordered O—H···N/N—H···O hydrogen bond is generated in which both H-atom sites are very close to the line N1···O1. In addition N2 in the cation at (x, y, z) acts as hydrogen-bond donor to the carboxylate O3 in the anion at ($1+x$, $\frac{1}{2}-y$, $-\frac{1}{2}+z$); thus a $C_2^2(12)$ chain that runs parallel to the [20$\bar{1}$] direction is generated by the *c*-glide plane at $y=\frac{1}{4}$. Two such chains, which are related to one another by centres of inversion and are thus antiparallel, run through each unit cell, and the [20$\bar{1}$] chains are linked into (102) sheets by the action of a single C—H···O hydrogen bond.

Atom C23 in the cation at (x, y, z) acts as hydrogen-bond donor, *via* H23*A*, to the carboxylate O4 in the anion at ($1-x$, $-y$, $1-z$), while C23 at ($1-x$, $-y$, $1-z$) in turn acts as donor to O4 at (x, y, z). In this manner a centrosymmetric $R_4^4(22)$ ring is produced, which is centred at ($\frac{1}{2}$, 0, $\frac{1}{2}$). The combination of this ring motif with the $C_2^2(12)$ chains generates the (102) sheets, which are built from $R_4^4(22)$ and $R_8^8(38)$ rings, both centrosymmetric, that alternate in checkerboard fashion (Fig. 15). There are no C—H···π(arene) hydrogen bonds in the structure of (6), thus the supramolecular structure defined by the direction-specific interactions is two dimensional.

3.3.5. Chains are linked by C—H···O hydrogen bonds into frameworks. *Single frameworks*. *Compound (7)*. In (7) (Fig. 16) the molecular components are both neutral, with no evidence for H-atom transfer from O to N. Both components lie across centres of inversion, and for the sake of convenience the diamine was centred at ($\frac{1}{2}$, $\frac{1}{2}$, $\frac{1}{2}$). The hydrogen bond within the asymmetric unit then requires the acid unit to be centred at ($\frac{1}{4}$, $-\frac{3}{4}$, 0). Propagation of the single O—H···N hydrogen bond by successive centres of inversion thus generates a $C_2^2(18)$ chain that runs parallel to the [152] direction (Fig. 17), while the action of the twofold axes generate similar chains that run parallel to [1$\bar{5}$2].

There are neither aromatic $\pi\cdots\pi$ stacking interactions nor C—H···π(arene) interactions present in the structure of (7) and the sole direction-specific interaction between components of different chains is a single, rather weak, C—H···O hydrogen bond, whose action is to link the [152] and [1$\bar{5}$2] chains into a continuous three-dimensional framework. In the reference cation centred at ($\frac{1}{2}$, $\frac{1}{2}$, $\frac{1}{2}$), which lies in a [152] chain,

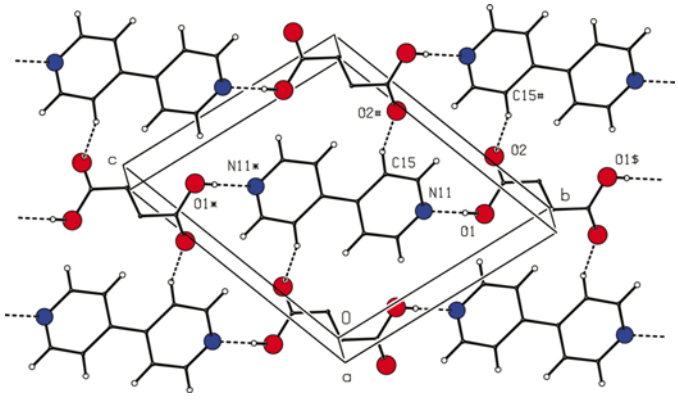

Figure 13
Part of the crystal structure of (5), which shows the formation of a (10$\bar{2}$) sheet built from alternating $R_4^4(14)$ and $R_4^4(28)$ rings. For the sake of clarity, the H atom bonded to C2 is omitted. The atoms marked with an asterisk (*), hash (#) or dollar sign ($) are at the symmetry positions ($1-x$, $1-y$, $1-z$), ($1-x$, $2-y$, $1-z$) and ($-1-x$, $2-y$, $-z$), respectively.

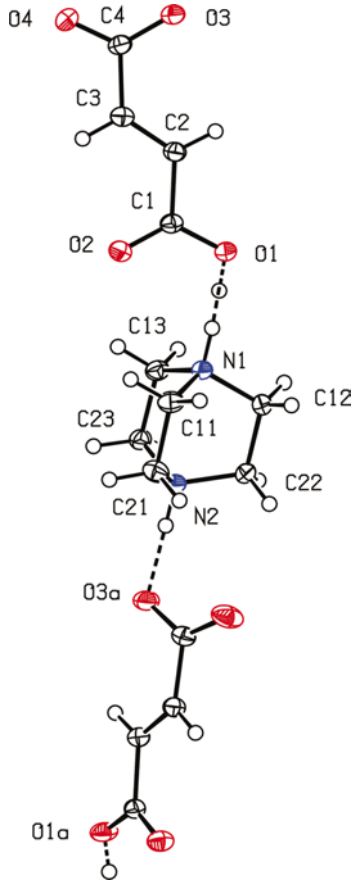

Figure 14
The components of (6) and the atom-labelling scheme. An additional anion is included in order to show the ordered and disordered hydrogen bonds that form the [20$\bar{1}$] chain. Displacement ellipsoids are drawn at the 30% probability level, and atoms marked with '*a*' are at the symmetry position ($1+x$, $\frac{1}{2}-y$, $-\frac{1}{2}+z$). For the sake of clarity, the unit-cell box is omitted.

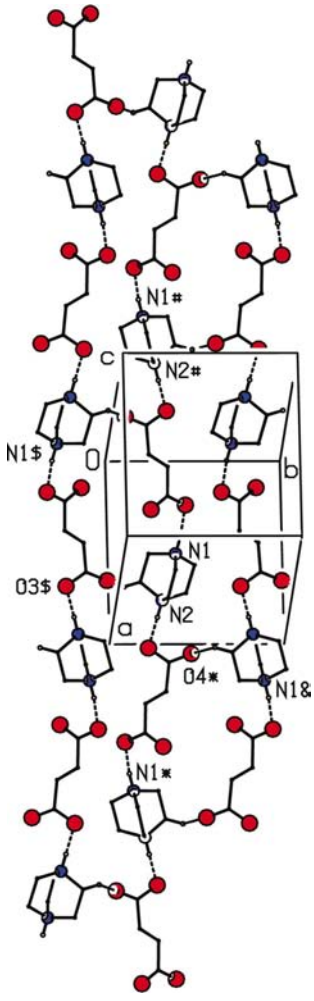

Figure 15
Part of the crystal structure of (6), which shows the formation of a (102) sheet built from alternating $R_4^4(22)$ and $R_8^8(38)$ rings. For the sake of clarity, the only H atom bonded to C shown is that involved in the hydrogen bonding depicted. The atoms marked with an asterisk (*), hash (#), dollar sign ($) or ampersand (&) are at the symmetry positions $(1 + x, \frac{1}{2} - y, -\frac{1}{2} + z)$, $(-1 + x, \frac{1}{2} - y, \frac{1}{2} + z)$, $(1 - x, -y, 1 - z)$ and $(2 - x, \frac{1}{2} + y, \frac{1}{2} - z)$, respectively.

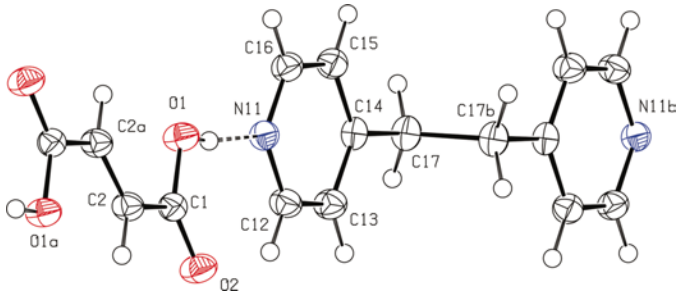

Figure 16
The components of (7) and the atom-labelling scheme. Displacement ellipsoids are drawn at the 50% probability level. The atoms marked '*a*' or '*b*' are at the symmetry positions $(\frac{1}{2} - x, -\frac{3}{2} - y, -z)$ and $(1 - x, 1 - y, 1 - z)$, respectively.

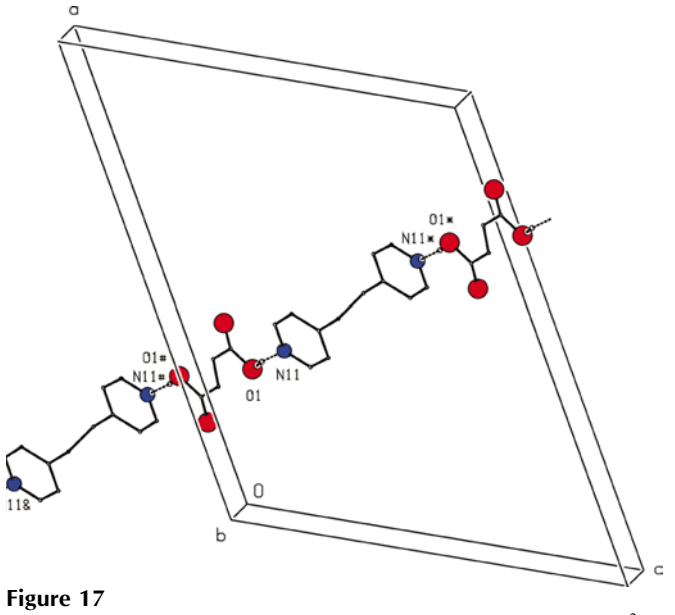

Figure 17
Part of the crystal structure of (7), which shows the formation of a $C_2^2(18)$ chain along [152]. For the sake of clarity, H atoms bonded to C are omitted. The atoms marked with an asterisk (*), hash (#) or ampersand (&) are at the symmetry positions $(1 - x, 1 - y, 1 - z)$, $(\frac{1}{2} - x, -\frac{3}{2} - y, -z)$ and $(-\frac{1}{2} + x, -\frac{5}{2} + y, -1 + z)$, respectively.

the C16 atoms at (x, y, z) and $(1 - x, 1 - y, 1 - z)$ act as hydrogen-bond donors, respectively, to atoms O1 in the anions at $(\frac{1}{2} - x, \frac{1}{2} + y, \frac{1}{2} - z)$ and at $(\frac{1}{2} + x, \frac{1}{2} - y, \frac{1}{2} + z)$. These anions lie in the $[1\bar{5}2]$ chains that pass through (0, 1, 0) and (1, 0, 1), respectively. Propagation of this single hydrogen bond suffices to link all of the chains into a continuous structure (Fig. 18).

Compound (8). Both molecular components in (8) are neutral and both lie in special positions: the diamine lies across a twofold rotation axis and the acid lies across a centre of inversion. With the axis selected as that along $(\frac{1}{2}, y, \frac{3}{4})$, the connected asymmetric unit (Fig. 19) requires the acid to lie across the inversion centre at $(\frac{3}{4}, \frac{1}{4}, \frac{1}{2})$. A single O—H···N hydrogen bond (Table 2) links the components into a $C(19)$ chain that runs parallel to the $[10\bar{1}]$ direction

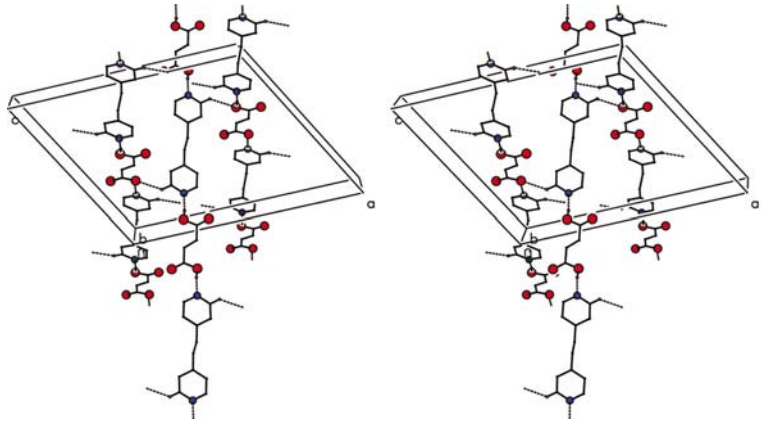

Figure 18
Stereoview of part of the crystal structure of (7), which shows the linking of the [152] and $[1\bar{5}2]$ chains into a continuous framework. For the sake of clarity, the only H atom bonded to C shown is that involved in the hydrogen bonding depicted.

and is defined by the symmetry elements across which the components lie (Fig. 20).

The $[10\bar{1}]$ chains are further linked by a single, rather weak, C—H···O hydrogen bond to form a continuous three-dimensional framework. Atom C16 at (x, y, z) acts as hydrogen-bond donor to the carboxyl O1 at ($\frac{3}{2}-x$, $\frac{1}{2}+y$, $\frac{3}{2}-z$), while C16 at ($\frac{3}{2}-x$, $\frac{1}{2}+y$, $\frac{3}{2}-z$) in turn acts as donor to O1 at (x, $1+y$, z); thus a $C(5)$ spiral chain that runs parallel to the [010] direction is generated by the 2_1 screw axis along ($\frac{3}{4}$, y, $\frac{3}{4}$) (Fig. 21). The propagation of this spiral-chain motif by the rotation and inversion symmetry elements across which the molecular components lie serves to link not only adjacent $[10\bar{1}]$ chains related by translation in the [010] direction, thereby forming a (101) sheet, but also adjacent $[10\bar{1}]$ chains related by the 2_1 axes. In this manner all of the $[10\bar{1}]$ chains are linked into a continuous bundle. However, neither C—H···π(arene) hydrogen bonds nor aromatic $\pi\cdots\pi$ stacking interactions are present in the structure of (8).

Compound (9). The 1:2 adduct, (9) (Fig. 22), that is formed between 2,2′-dipyridylamine and maleic acid is a salt $[\{(C_{10}H_9N_3)H\}^+]\cdot[(C_4H_{3.5}O_4)^{-0.5}]_2$. The cation, which contains the usual intramolecular N—H···N hydrogen bond typical of this species, is disordered across a centre of inversion: that at ($\frac{1}{2}$, $\frac{1}{2}$, $\frac{1}{2}$) is chosen for the sake of convenience. The anion contains the same type of intramolecular O—H···O hydrogen bond as is observed in the $(C_4H_3O_4)^-$ anions in (1) and (2), but in (9) there is an additional H-atom site, which has 0.5 occupancy and is associated with O4. Pairs of anions are linked across centres of inversion by disordered O—H···O hydrogen bonds: of the two possible H-atom sites between a centrosymmetric pair of adjacent O4 sites, only one can be occupied. Within the asymmetric unit, the cations and anions are linked by a combination of N—H···O and C—H···O hydrogen bonds. For one orientation of the cation, there is the N1—H1···O1 hydrogen bond (Fig. 22), while for the other orientation, O1 is an acceptor from N11 and O2 is an acceptor from C13 at ($1-x$, $1-y$, $1-z$). While some of these individual hydrogen bonds may be rather weak (Table 2), they act cooperatively. With the disordered cation centred at ($\frac{1}{2}$, $\frac{1}{2}$, $\frac{1}{2}$), the connectivity of the asymmetric unit means that the disordered O—H···O hydrogen bonds are centred at (0, 2, $\frac{1}{2}$). Propagation by inversion of the intermolecular hydrogen bonds then generates a $C_3^3(18)$ chain that runs parallel to the $[1\bar{3}0]$ direction.

The action of the 2_1 screw axes on the $[1\bar{3}0]$ chain generates a similar chain that runs parallel to [103], and chains that run in these two directions alternate along [001] (Fig. 23). The criss-cross chains are rather weakly linked by one further C—H···O hydrogen bond to form a single three-dimensional

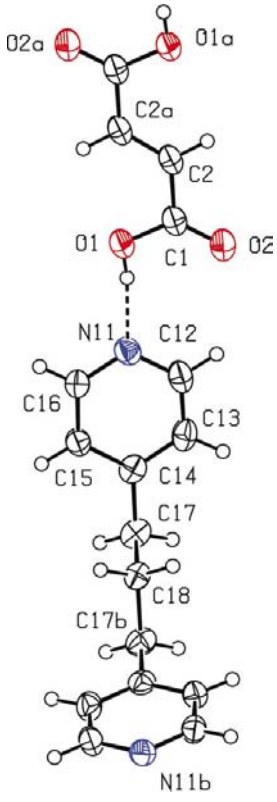

Figure 19
The components of (8) and the atom-labelling scheme. Displacement ellipsoids are drawn at the 50% probability level. The atoms marked with '*a*' or '*b*' are at the symmetry positions ($\frac{3}{2}-x$, $\frac{1}{2}-y$, $1-z$) and ($1-x$, y, $\frac{3}{2}-z$), respectively.

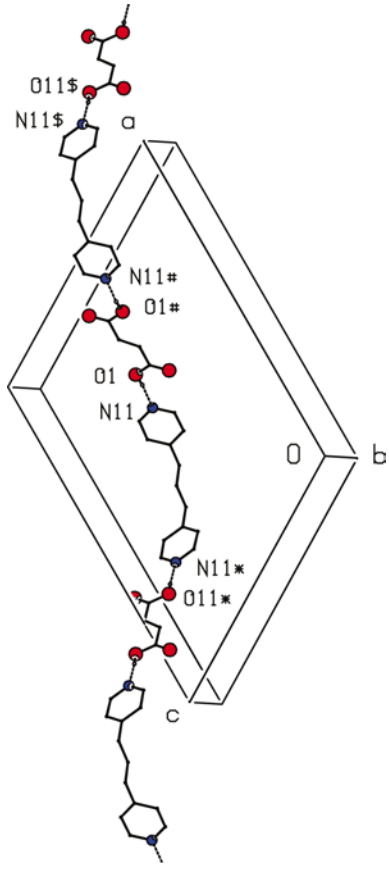

Figure 20
Part of the crystal structure of (8), which shows the formation of a $[10\bar{1}]$ chain. For the sake of clarity, H atoms bonded to C are omitted. The atoms marked with an asterisk (*), hash (#) or dollar sign ($) are at the symmetry positions ($1-x$, y, $\frac{3}{2}-z$), ($\frac{3}{2}-x$, $\frac{1}{2}-y$, $1-z$) and ($\frac{1}{2}+x$, $\frac{1}{2}-y$, $-\frac{1}{2}+z$), respectively.

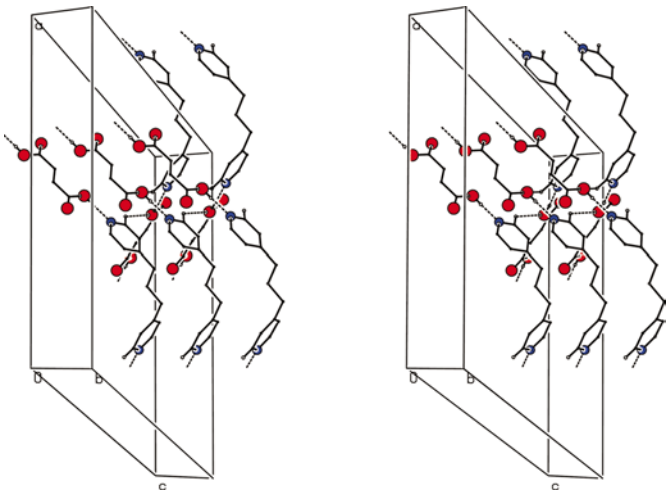

Figure 21
Stereoview of part of the crystal structure of (8), which shows the formation of a $C(5)$ chain along [010]. For the sake of clarity, the only H atom bonded to C shown is that involved in the hydrogen bonding depicted.

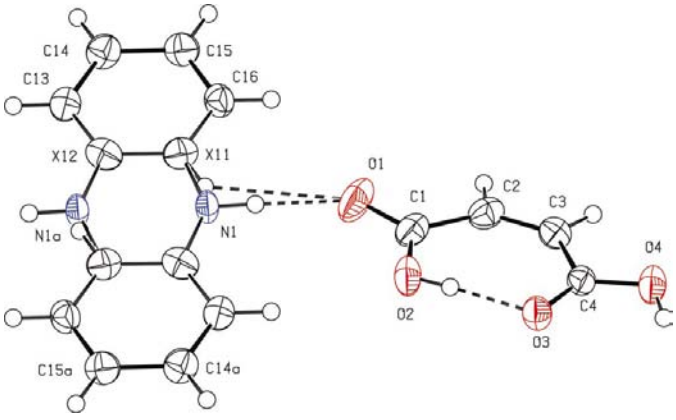

Figure 22
The components of (9) and the atom-labelling scheme. Displacement ellipsoids are drawn at the 50% probability level. In the cation, N1 has occupancy 0.5, the sites denoted *X*11 and *X*12 are each occupied by (0.5 C + 0.5 N), and the H atoms associated with N1, N11 and O4 all have occupancy 0.5. The atoms marked '*a*' are at the symmetry position $(1-x, 1-y, 1-z)$.

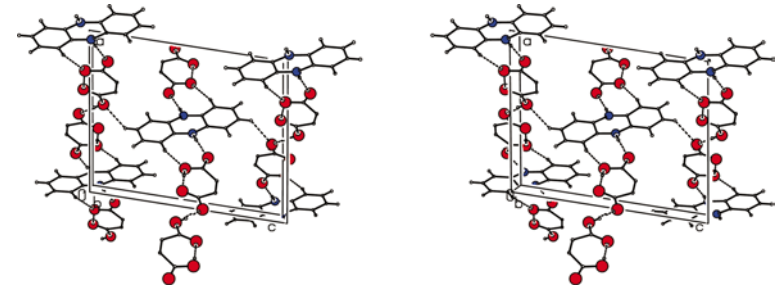

Figure 23
Stereoview of part of the crystal structure of (9), which shows the linking of the [130] and [1$\bar{3}$0] chains into a continuous framework.

framework. C15 in the cation at (x, y, z), which forms part of a [1$\bar{3}$0] chain, acts as hydrogen-bond donor to the carboxylate O4 in the anion at $(\frac{1}{2}-x, -\frac{3}{2}+y, \frac{3}{2}-z)$, which lies in the adjacent [130] chain. Propagation of this hydrogen bond by inversion links the chain along [001], while propagation *via* the 2_1 screw axes generates a $C_2^2(12)$ chain along [010]. The combination of [010], [001], [130] and [1$\bar{3}$0] chains suffices to generate a single three-dimensional framework.

Compound (10). Compound (10) contains monoprotonated HMTA cations $[\{(C_6H_{12}N_4)H\}^+]$ and an approximately 3:1 ratio of fumarate and succinate monoanions $(C_4H_3O_4)^-$ and $(C_4H_5O_4)^-$. The structural roles of the two anion types are identical because of the very close similarity between the O-atom sites occupied by the two types. Hence we discuss the structure only in terms of the major anion, fumarate. The supramolecular structure differs from those in (7)–(9) in that the hard hydrogen bonds generate a chain of anions from which the cations are pendent, rather than a chain of alternating cations and anions. In the fumarate anion at (x, y, z), the carboxyl O4 acts as hydrogen-bond donor to the carboxylate O1 in the corresponding anion at $(-1+x, y, z)$; thus a $C(7)$ chain that runs parallel to the [100] direction is generated by translation. Within the asymmetric unit, N1 acts as hydrogen-bond donor to the carboxyl O1, so that there is a cation pendent from each anion in the [100] chain (Fig. 24).

Four of these chains run through each unit cell, and they are linked into a three-dimensional framework by two C—H···O hydrogen bonds. In these the donors are both in the cation: C12, which is adjacent to the protonated N1, and C34, which is adjacent to the iminium centres N3 and N4 (see Scheme II). Atom C34 in the cation at (x, y, z) acts as hydrogen-bond donor, *via* H34*A*, to the carboxyl O3 in the anion at $(2-x, 1-y, 1-z)$; thus an $R_4^4(24)$ ring that is centred at $(1, \frac{1}{2}, \frac{1}{2})$ is generated (Fig. 25). This four-component dimer can conveniently be taken as the basic building block for the substructure that is dependent on C—H···O hydrogen bonds.

In the second C—H···O hydrogen bond, atom C12 in the cation at (x, y, z), which forms part of the dimer centred at $(1, \frac{1}{2}, \frac{1}{2})$, acts as hydrogen-bond donor, *via* H12*A*, to the carboxyl O4 in the anion at $(1-x, \frac{1}{2}+y, \frac{1}{2}-z)$, which is part of the dimer centred at (0, 1, 0). Similarly, O4 in the anion at (x, y, z) accepts a hydrogen bond from C12 in the cation at $(1-x, -\frac{1}{2}+y, \frac{1}{2}-z)$, which lies in the dimer centred at (0, 0, 0). Propagation of this hydrogen bond by inversion further links the dimer centred at $(1, \frac{1}{2}, \frac{1}{2})$ to those centred at (2, 0, 1) and (2, 1, 1); hence a sheet parallel to (102) (Fig. 26) is generated. The combination of (102) sheets and [100] chains (Fig. 24) suffices to generate a single three-dimensional framework.

A double framework, compound (11). In (11) (Fig. 27), both components are neutral with no evidence for any transfer of H atoms from O to N. Two nearly linear N—H···O hydrogen bonds (Table 2) link the molecules into chains. The carboxyl O1 acts as hydrogen-bond donor to N11 within the asymmetric unit, and this hydrogen

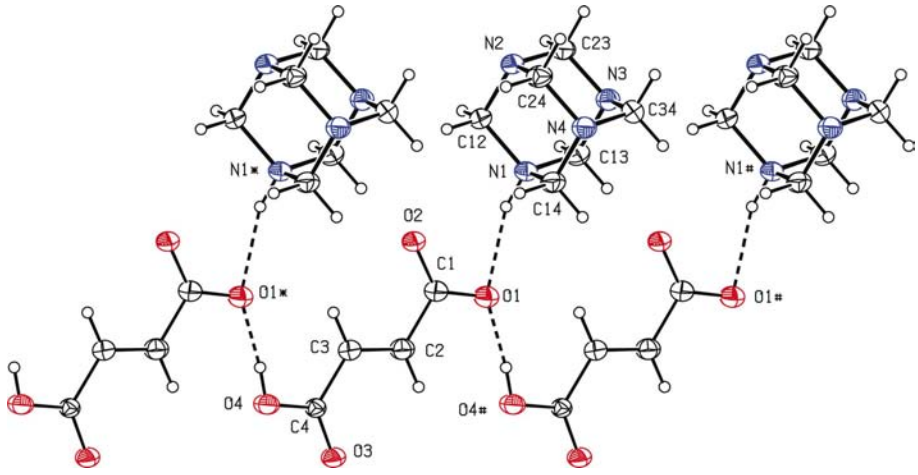

Figure 24
The principal components of (10) and the atom-labelling scheme. The formation of an anion chain along [100] with pendent cations is shown. Displacement ellipsoids are drawn at the 30% probability level. For the sake of clarity, the succinate component (C41—C44, O41—O44) and the unit-cell box are omitted. The atoms marked with an asterisk (*) or a hash (#) are at the symmetry positions $(-1 + x, y, z)$ and $(1 + x, y, z)$, respectively.

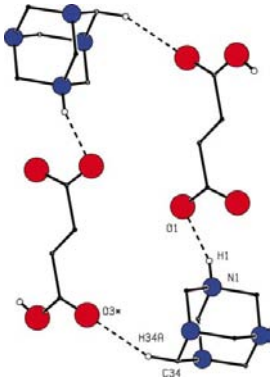

Figure 25
Part of the crystal structure of (10), which shows the formation of a centrosymmetric $R_4^4(24)$ dimer. For the sake of clarity, the succinate component and the unit-cell box are omitted, and the only H atom bonded to C shown is that involved in the hydrogen bonding depicted. The atoms marked with an asterisk (*) are at the symmetry position $(2 - x, 1 - y, 1 - z)$.

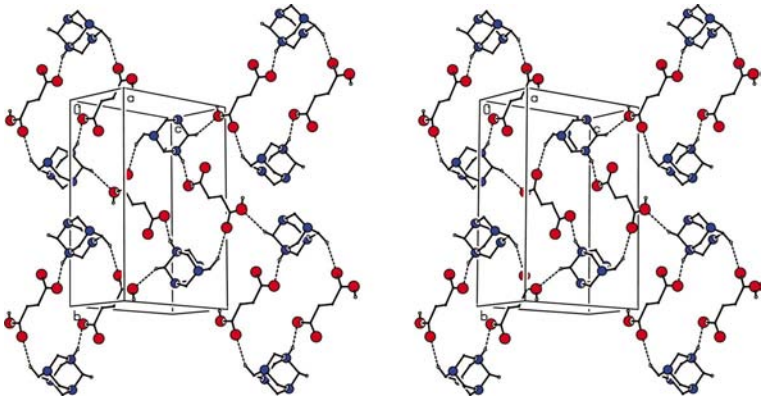

Figure 26
Stereoview of part of the crystal structure of (10), which shows the formation of a (102) sheet. For the sake of clarity, the succinate component is omitted and the only H atom bonded to C shown is that involved in the hydrogen bonding depicted.

bond is reinforced by the action of C16 as donor to O2, also within the asymmetric unit; thus the nearly planar $R_2^2(7)$ motif, which is occasionally encountered in pyridines, is produced. The carboxyl O3 in the same acid unit at (x, y, z) acts as hydrogen-bond donor to N21 in the diamine at $(\frac{1}{2} + x, 2 - y, z)$. Propagation of these two hydrogen-bond motifs produces a $C_2^2(12)$ chain that runs parallel to the [100] direction and is generated by the *a*-glide plane at $y = 1.0$ (Fig. 28). A single C—H···O hydrogen bond suffices to generate a three-dimensional continuum from the [100] chains.

Atom C14 in the diamine at (x, y, z) acts as hydrogen-bond donor to the carboxyl O4 in the acid at $(\frac{1}{2} - x, -1 + y, \frac{1}{2} + z)$, while C14 at $(\frac{1}{2} - x, -1 + y, \frac{1}{2} + z)$ in turn acts as donor to O4 at $(x, -2 + y, 1 + z)$. In this manner a $C_2^2(12)$ chain is generated that runs parallel to the $[0\bar{2}1]$ direction. The action of the 2_1 screw axis parallel to [001] generates a similar chain parallel to [021] (Fig. 29), and the combination of the [100], [021] and $[0\bar{2}1]$ chains generates a three-dimensional framework that, however, encompasses only half of the unit-cell contents: there are thus two interwoven frameworks.

3.4. General comparison of the maleic and fumaric acid adducts

In this section we briefly compare the structural characteristics of the cognate pairs of adducts that maleic and fumaric acids form with a common amine.

3.4.1. Bipyridyl adducts. The 1:2 adduct, (2), that is formed between 4,4′-bipyridyl and maleic acid is a salt with the cation lying across a twofold axis in *C*2/*c*. In (2) the single N—H···O hydrogen bond generates a three-ion aggregate; these aggregates are linked by multiple C—H···O hydrogen bonds into a three-dimensional framework. By contrast, the adduct, (5), that is formed between 4,4′-bipyridyl and fumaric acid has 1:1 stoichiometry, both

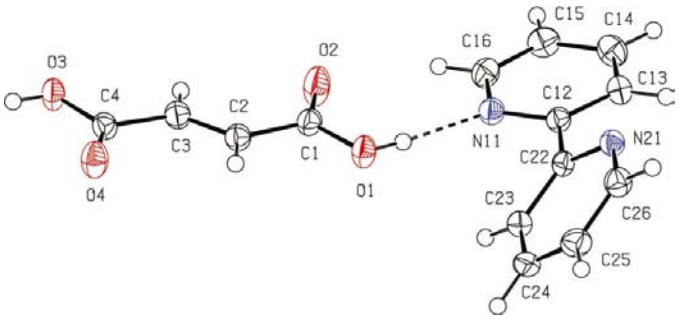

Figure 27
The components of (11) and the atom-labelling scheme. Displacement ellipsoids are drawn at the 50% probability level.

components are neutral and both lie across inversion centres in $P\bar{1}$. A single O—H···N hydrogen bond generates chains, and the chains are linked into sheets by a single C—H···O hydrogen bond. In the analogous 1:1 adduct, (11), that is formed by 2,2′-bipyridyl with fumaric acid, both components are again neutral, as in (5), but both lie in general positions, despite the fact that both could in principle lie on sites with symmetry as high as C_{2h} (2/*m*), while the diamine could also adopt C_{2v} (*mm*2) symmetry. Two distinct O—H···N hydrogen bonds generate chains similar to those in (5), but in (11) the single C—H···O hydrogen bond links the chain into two interwoven frameworks.

3.4.2. Adducts of chain-extended bipyridyls. With maleic acid, 1,2-bis(4-pyridyl)ethane forms a 1:2 salt, (1), in which the cation lies across a centre of inversion. The single N—H···O hydrogen bond generates a three-ion aggregate, as in (2), but in (1) the overall supramolecular structure is only two-dimensional, despite the occurrence of multiple C—H···O hydrogen bonds. In the 1:1 adduct of 1,2-bis(4-pyridyl)ethane and fumaric acid, (7), both components are neutral and both lie across inversion centres, although in *C*2/*c*, as opposed to $P\bar{1}$, which is found for the analogous adduct (5) formed by 4,4′-bipyridyl. As in (5), the single O—H···N hydrogen bond in (7) generates chains but, because of the presence of the twofold rotation axes in (7), the single C—H···O hydrogen bond now generates a three-dimensional supramolecular structure, rather than the two-dimensional structure in (5).

Closely related to (7) is the 1:1 adduct, (8), that is formed between 4,4′-trimethylenedipyridine and fumaric acid. Here both components are neutral, and the adduct crystallizes in *C*2/*c* with the acid component lying across a centre of inversion, as in (7). However, the presence of a trimethylene spacer unit between the two pyridine rings of the diamine prevents this diamine from lying across a centre of inversion. Instead, the diamine lies across a twofold rotation axis and provides an interesting example of a symmetry change that is enforced by a simple change in molecular constitution. As in (7), however, the single O—H···N hydrogen bond in (8) generates chains that consist of alternating diamine and acid units, and these chains are linked by a single C—H···O hydrogen bond; again, a three-dimensional framework is formed.

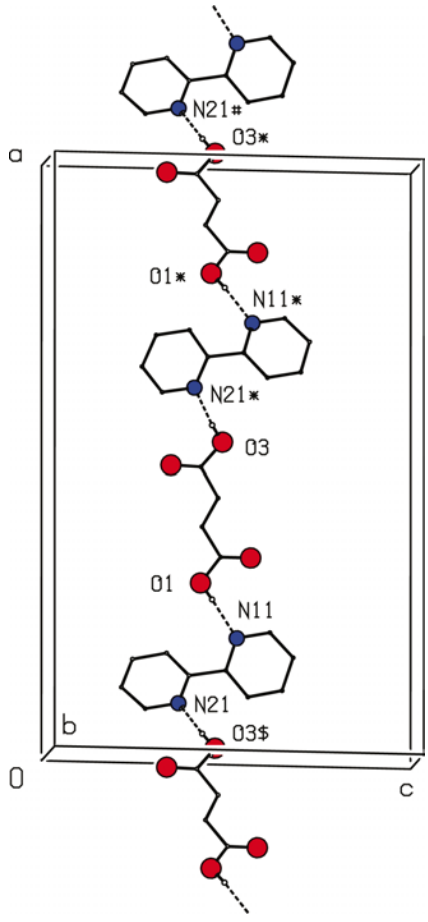

Figure 28
Part of the crystal structure of (11), which shows the formation of a $C_2^2(12)$ chain along [100]. For the sake of clarity, H atoms bonded to C are omitted. The atoms marked with an asterisk (*), hash (#) or dollar sign ($) are at the symmetry positions $(\frac{1}{2}+x, 2-y, z)$, $(1+x, y, z)$ and $(-\frac{1}{2}+x, 2-y, z)$, respectively.

3.4.3. Adducts of 2,2′-dipyridylamine. The maleic and fumaric acid adducts of the bipyridyl species (discussed in §§3.4.1 and 3.4.2) have a number of features in common:

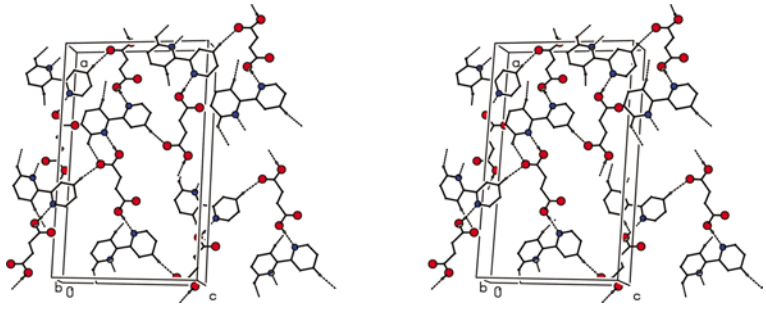

Figure 29
Stereoview of part of the crystal structure of (11), which shows the formation of the [021] and [0$\bar{2}$1] chains that link the [100] chains. For the sake of clarity, the only H atoms bonded to C shown are those involved in the hydrogen bonding depicted.

the maleic acid adducts are salts of the type $[\{(\text{diamine})H_2\}^{2+}]\cdot[(C_4H_3O_4)^-]$, while the 1:1 fumaric acid adducts contain only neutral components. The adducts (3) and (9) that are formed with 2,2′-bipyridyl have very different constitutions from the adducts of the bipyridyls, even though the stoichiometries are similar to those in the bipyridyl adducts. Firstly, both (3) and (9) are salts that contain the monoprotonated cation $[\{(C_{10}H_9N_3)H\}^+]$, in which there is an intramolecular N—H···N hydrogen bond. Secondly, while the 1:1 fumaric acid adduct (3) contains the simple anion $[(C_4H_3O_4)^-]$, the 1:2 maleic acid adduct contains the anion $[(C_4H_{3.5}O_4)^{-0.5}]$ with disordered H atoms. Thirdly, the hard hydrogen bonds in (9) generate continuous chains rather than the finite three-ion aggregates found in (1) and (2), while in (3) the hard hydrogen bonds generate molecular ladders rather than the simple chains found in (5), (7), (8) and (11).

3.4.4. Adducts of cage amines. The 1:2 adduct formed between DABCO and maleic acid (Sun & Jin, 2002) has a constitution and overall supramolecular structure very similar to those formed by bipyridyls with maleic acid. The DABCO-fumaric acid system is unusual in that two adducts have been isolated: a 1:2 adduct (4) and a 1:1 adduct (6). Compound (4) is the only 1:2 adduct of fumaric acid found in this study. The 1:2 adduct is a salt of type $[\{(\text{diamine})H_2\}^{2+}]\cdot[(C_4H_3O_4)^-]_2$, in which pairs of *C*(7) anion chains that are related by a twofold rotation axis are linked by the cations into a molecular ladder: this may be compared with the molecular ladder in (3) where the pairs of *C*(7) chains in the ladder are related by inversion rather than by rotation. The 1:1 adduct (6), by contrast, has a supramolecular structure that is more typical of those found with the bipyridyls, despite the partial H-atom transfer from O to N in (6), in that chains generated by the hard hydrogen bonds are further linked by a single C—H···O hydrogen bond into sheets. The 1:1 adduct of HMTA with fumaric acid, (10), has a supramolecular structure unlike any other studied here, with $[\{(C_6H_{12}N_4)H\}^+]$ cations pendent from a *C*(7) anion chain.

4. Concluding comments

The structures of the adducts reported and analysed here indicate that the adducts formed by the isomeric pair of acids, maleic and fumaric acid, with simple organic diamines generally (but not reliably) have amine:acid molar ratios of 2:1 and 1:1, respectively. However, the adducts formed by 1,4-diazabicyclo[2.2.2]octane, (4) and (6), suffice to call even this simple generalization into question. Likewise the simple pattern of chains of alternating amine and acid units in the fumaric acid systems sees exceptions in (4) and (10) where the supramolecular structures are dominated by chains formed solely by the acid units. For the dozen compounds discussed here, it would be difficult to make reliable predictions (at least using qualitative reasoning) of the detailed structure of any one of them, even if the detailed structures of all of the remainder are known and despite the chemical simplicity of the molecular building blocks employed.

X-ray data were collected at the University of Toronto using a Nonius Kappa-CCD diffractometer purchased with funds from NSERC Canada.

References

Allen, F. H., Kennard, O., Watson, D. G., Brammer, L., Orpen, A. G. & Taylor, R. (1987). *J. Chem. Soc. Perkin Trans.* **2**, pp. S1–S19.
Bednowitz, A. L. & Post, B. (1966). *Acta Cryst.* **21**, 566–571.
Bernstein, J., Davis, R. E., Shimoni, L. & Chang, N.-L. (1995). *Angew. Chem. Int. Ed. Engl.* **34**, 1555–1573.
Braga, D., Grepioni, F., Biradha, K., Pedireddi, V. R. & Desiraju, G. R. (1995). *J. Am. Chem. Soc.* **117**, 3156–3166.
Brock, C. P. & Dunitz, J. D. (1994). *Chem. Mater.* **6**, 1118–1127.
Brown, C. J. (1966). *Acta Cryst.* **21**, 1–5.
Chatterjee, S., Pedireddi, V. R. & Rao, C. N. R. (1998). *Tetrahedron Letts.* **39**, 2843–2846.
Coupar, P. I., Glidewell, C. & Ferguson, G. (1997). *Acta Cryst.* B**53**, 521–533.
Farrell, D. M. M., Ferguson, G., Lough, A. J. & Glidewell, C. (2002*a*). *Acta Cryst.* B**58**, 272–288.
Farrell, D. M. M., Ferguson, G., Lough, A. J. & Glidewell, C. (2002*b*). *Acta Cryst.* B**58**, 530–544.
Ferguson, G. (1999). *PRPKAPPA – A WordPerfect* 5.1 *Macro to Formulate and Polish CIF Format Files from the SHELXL*97 *Refinement of Kappa-CCD Data.* University of Guelph, Canada.
Ferguson, G., Coupar, P. I. & Glidewell, C. (1997). *Acta Cryst.* B**53**, 513–520.
Ferguson, G., Glidewell, C., Gregson, R. M., Meehan, P. R. & Patterson, I. L. J. (1998). *Acta Cryst.* B**54**, 151–161.
Flack, H. D. (1983). *Acta Cryst.* A**39**, 876–881.
Flack, H. D. & Bernardinelli, G. (2000). *J. Appl. Cryst.* **33**, 1143–1148.
Glidewell, C., Ferguson, G., Gregson, R. M. & Lough, A. J. (1999). *Acta Cryst.* C**55**, 2133–2136.
James, M. N. G. & Williams, G. J. B. (1974). *Acta Cryst.* B**30**, 1249–1257.
Lavender, E. S., Ferguson, G. & Glidewell, C. (1999). *Acta Cryst.* C**55**, 430–432.
Nonius (1997). *Kappa-CCD Server Software.* Windows 3.11 Version. Nonius B. V., Delft, The Netherlands.
Otwinowski, Z. & Minor, W. (1997). *Methods Enzymol.* **276**, 307–326.
Shahat, M. (1952). *Acta Cryst.* **5**, 763–768.
Sheldrick, G. M. (1997*a*). *SHELXL*97. *Program for the Refinement of Crystal Structures.* University of Göttingen, Germany.
Sheldrick, G. M. (1997*b*). *SHELXS*97. *Program for the Solution of Crystal Structures.* University of Göttingen, Germany.
Spek, A. L. (2002). *PLATON. Molecular Geometry and Graphics Program.* Version of June 2002. University of Utrecht, The Netherlands.
Sun, C. R. & Jin, Z. M. (2002). *Acta Cryst.* C**58**, o600–o601.
Wilson, A. J. C. (1976). *Acta Cryst.* A**32**, 994–996.
Yardley, K. (1925). *Philos. Mag.* **50**, 864–878.